

CoIFNet: A Unified Framework for Multivariate Time Series Forecasting with Missing Values

Kai Tang, Ji Zhang*, Hua Meng, Minbo Ma, Qi Xiong, Fengmao Lv, Jie Xu, Tianrui Li

Abstract—Multivariate time series forecasting (MTSF) is a critical task with broad applications in domains such as meteorology, transportation, and economics. Nevertheless, pervasive missing values caused by sensor failures or human errors significantly degrade forecasting accuracy. Prior efforts usually employ an impute-then-forecast paradigm, leading to suboptimal predictions due to error accumulation and misaligned objectives between the two stages. To address this challenge, we propose the Collaborative Imputation-Forecasting Network (CoIFNet), a novel framework that unifies imputation and forecasting to achieve robust MTSF in the presence of missing values. Specifically, CoIFNet takes the observed values, mask matrix and timestamp embeddings as input, processing them sequentially through the Cross-Timestep Fusion (CTF) and Cross-Variate Fusion (CVF) modules to capture temporal dependencies that are robust to missing values. We provide theoretical justifications on how our CoIFNet learning objective improves the performance bound of MTSF with missing values. Through extensive experiments on challenging MTSF benchmarks, we demonstrate the effectiveness and computational efficiency of our proposed approach across diverse missing-data scenarios, e.g., CoIFNet outperforms the state-of-the-art method by **24.40%** (**23.81%**) at a point (block) missing rate of 0.6, while improving memory and time efficiency by $4.3\times$ and $2.1\times$, respectively. Our code is available at: <https://github.com/KaiTang-eng/CoIFNet>.

Index Terms—Data mining, multivariate time series forecasting, missing values, one-stage time series forecasting

1 INTRODUCTION

MULTIVARIATE time series forecasting (MTSF) plays an important role in various domains, including meteorology [1], traffic [2], economics [3] and so on. By modeling complex temporal dependencies and inter-variate correlations, advanced MTSF methods [4], [5], [6] have demonstrated significant capabilities in predicting critical metrics and anticipating future trends. Despite these significant advances, the practical deployment of MTSF models encounters a critical limitation: most existing approaches necessitate complete time series data, with observations available for all variates at each timestep. This assumption may not hold in real-world scenarios, as time series data collected in practical applications are often inherently incomplete, frequently exhibiting missing observations due to sensor failures, communication interruptions, data corruption, or limited resources [7], [8], [9], [10].

Previous methods [11], [12] generally adopt an impute-then-forecast pipeline, treating imputation and forecasting as distinct, sequential steps. This two-stage framework leads to suboptimal predictions due to error propagation and misaligned optimization objectives. To address this limitation, various one-stage approaches have been proposed. One line of research formulates MTSF with missing data as an imputation task, where the forecasting window is treated

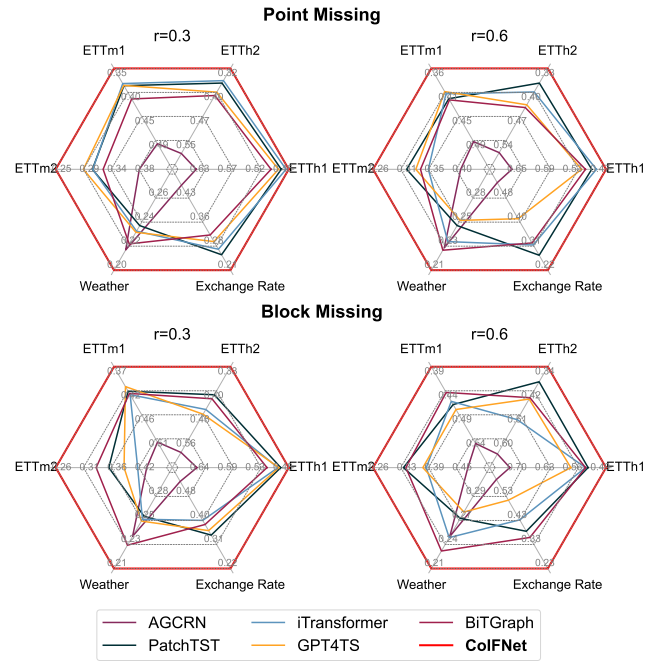


Fig. 1: Performance comparison between our CoIFNet approach and state-of-the-art multivariate time series forecasting (MTSF) methods on six real-world datasets under different missing-data scenarios.

as a block of missing values that need to be imputed [13], [14], [15]. In contrast, the recently proposed BiTGraph approach [16] performs forecasting directly on incomplete time series by leveraging mask-informed adaptive graphs to address missing values. While these methods derive fully observed forecasting values through a single imputation or

- Kai Tang, Ji Zhang, Qi Xiong, Fengmao Lv and Tianrui Li are with the School of Computing and Artificial Intelligence, Southwest Jiaotong University, Chengdu, China. E-mail: jizhang.jim@gmail.com. *Ji Zhang is the corresponding author.
- Hua Meng is with the School of Mathematics, Southwest Jiaotong University, Chengdu, China. Email: menghua@swjtu.edu.cn.
- Minbo Ma is with the Institute Carbon Neutrality, Tsinghua University, P.R. China. Email: minbo46.ma@gmail.com.
- Jie Xu is with the White Rose Grid e-Science Centre, University of Leeds, England. Email: J.Xu@leeds.ac.uk.

forecasting step, they overlook the complementary roles of imputation and forecasting, failing to leverage their mutual benefits for enhanced performance. This highlights a critical open question in MTSF:

Can imputation and forecasting be unified within a single framework to achieve robust time series forecasting in the presence of missing data?

In this work, we answer the question by proposing the **Collaborative Imputation-Forecasting Network (CoIFNet)**. **Technically**, CoIFNet first develops a Reversible Observed-value Normalization (RevON) module to mitigate data distribution shifts across time steps within the input lookback window. Then, the normalized observed values along with the corresponding mask matrix and timestamp embeddings are processed by sequential Cross-Timestep Fusion (CTF) and Cross-Variate Fusion (CVF) modules to capture temporal dependencies robust to missing values. At the end, the output series representations of the two sequential modules are projected to the original data space, where an imputation loss \mathcal{L}_I and a forecasting loss \mathcal{L}_F are built for joint training. **Theoretically**, we provide formal justifications grounded in the concept of mutual information [17], proving how the CoIFNet learning objective enhances the performance bound for MTSF with missing data. **Empirically**, we conduct extensive experiments on six real-world datasets across diverse missing-data scenarios (i.e., point missing and block missing), demonstrating CoIFNet’s superior performance and computational efficiency compared with state-of-the-arts, as presented in Fig. 1 and Fig. 7.

To summarize, the main contributions of this work are threefold:

- We propose CoIFNet, which unifies imputation and forecasting into a single framework to achieve robust MTSF in the presence of missing values.
- We theoretically demonstrate the superiority of our one-stage CoIFNet framework over traditional two-stage approaches for handling missing values in time series forecasting.
- Extensive experiments on six challenging real-world datasets demonstrate the effectiveness and computational efficiency of our proposed approach across diverse missing-data scenarios.

The remainder of this paper is organized as follows. Section 2 reviews related work. Section 3 introduces our proposed CoIFNet method. Section 4 provides a theoretical analysis of CoIFNet, while Section 5 presents and discusses the experimental results. Section 6 concludes the paper. Additional experimental results are included in the Appendix.

2 RELATED WORK

This section reviews existing multivariate time series forecasting (MTSF) methods designed for complete data, as well as representative approaches for handling missing values.

2.1 Multivariate Time Series Forecasting

MTSF has evolved from traditional statistical methods like ARIMA [18], [19] to sophisticated deep learning architectures [20], [21]. Graph-based methods have emerged as

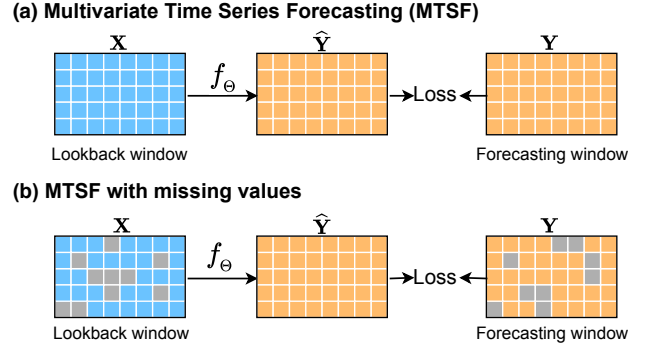


Fig. 2: Illustrations of Multivariate Time Series Forecasting (MTSF) with complete data (a) and with missing data (b). The blue block and orange block represent the *lookback window* and *forecasting window*, respectively, with gray regions within each block indicating missing values.

particularly effective approaches for multivariate scenarios. AGCRN [22] and MTGNN [23] construct adaptive graphs to model complex variate dependencies, demonstrating the importance of capturing both temporal dynamics and inter-variate relationships. Recent research has revealed counterintuitive insights about architectural complexity. DLinear [24] shows that linear models with proper decomposition can outperform sophisticated methods, challenging assumptions about complexity and performance. Additionally, STID [25] demonstrates that auxiliary timestamp features significantly enhance forecasting accuracy by capturing seasonal dynamics. Transformer-based models represent a significant breakthrough in long-sequence forecasting through self-attention mechanisms [26], [27]. PatchTST [28] introduces patching techniques that improve efficiency and performance, while iTransformer [5] employs inverted attention to treat variates as tokens rather than timesteps. The recent emergence of Large Language Models has introduced novel paradigms, with GPT4TS [29] exploring how pre-trained language models can be adapted for time series analysis through prompt-based forecasting approaches [30], [31]. Despite these advances, existing methods assume complete observations at each timestep. When facing missing values, most approaches resort to simple preprocessing strategies like mean imputation, creating suboptimal two-stage pipelines that fail to jointly optimize imputation and forecasting objectives.

2.2 MTSF with Missing Values

Traditional approaches follow a two-stage paradigm that separates imputation and forecasting into sequential tasks. Statistical methods perform simple interpolation before applying forecasting models. Learning-based imputation methods like BRITS [14], PriSTI [32], and SAITS [33] use RNNs or attention mechanisms to recover missing values by modeling temporal dependencies. However, this decoupled framework suffers from error propagation and misaligned optimization objectives between imputation and forecasting stages. Recent efforts have explored end-to-end solutions to address these limitations. GRU-D [34] incorporates decay mechanisms for missing values but was originally designed for classification and lacks explicit forecasting

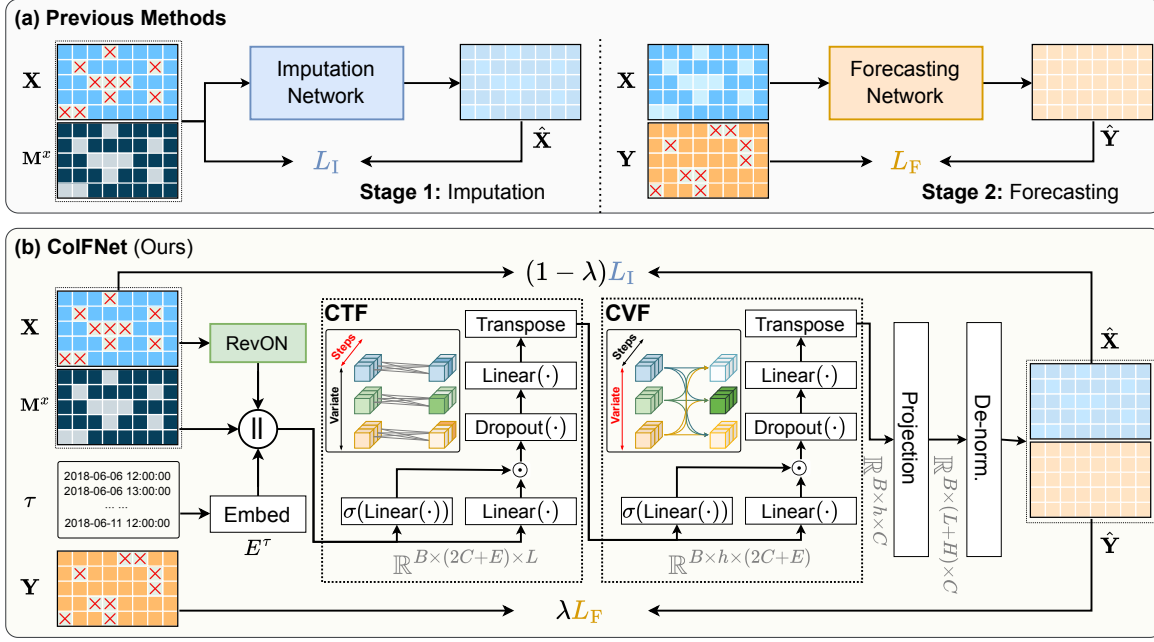


Fig. 3: **Illustration of CoIFNet.** Unlike previous methods that employ an input-then-forecast paradigm, CoIFNet formulates imputation and forecasting in a unified framework to achieve robust MTSF with missing values. First, CoIFNet introduces a Reversible Observed-value Normalization (RevON) module to mitigate data distribution shifts across time steps within the input lookback window \mathbf{X} . Next, the normalized values together with mask matrix \mathbf{M}^x and temporal embeddings E^τ are fed into the sequential Cross-Timestep Fusion (CTF) and Cross-Variate Fusion (CVF) modules to learn temporal dependencies along the time step and variate dimensions. Finally, the output series representations are projected to the original data space, where an imputation loss \mathcal{L}_I and a forecasting loss \mathcal{L}_F are developed based on the de-normalized representations $\hat{\mathbf{X}}$ and $\hat{\mathbf{Y}}$ as well as the input lookback window \mathbf{X} and forecasting window (ground truth) \mathbf{Y} .

optimization. Neural ODE approaches [35], [36] naturally handle irregular sampling but suffer from computational complexity and limited exploitation of temporal patterns. More recent methods attempt unified treatment of missing values and forecasting. CSDI [13] reformulates forecasting as an imputation task using diffusion models, but exhibits discrepancy between training and inference stages. Wang et al. [37] demonstrate that aligning imputation with forecasting objectives can significantly improve performance. Although existing imputation-based approaches [13], [14], [15] can reconstruct complete inputs for forecasting, they fail to harness the full predictive potential of historical supervision signals. BitGraph [16] proposes missing-aware adaptive graph construction but underutilizes temporal information and incurs high computational costs. S4M [38] integrates missing data handling into the structured state space sequence (S4) model architecture, effectively capturing the underlying temporal and multivariate dependencies. Although many one-stage forecasting models incorporate additional components to better utilize observed values, they often overlook the complementary roles of imputation and forecasting, thereby failing to leverage their mutual benefits for enhanced performance. In addition, they typically require separate training of models for different miss rates, which limits their robustness [39], [40], [41].

3 METHODOLOGY

In this section, we introduce the Collaborative Imputation-Forecasting Network (CoIFNet), a one-stage MTSF frame-

TABLE 1: Key notations used in this paper

Notions	Description
f_Θ	Neural network with parameters Θ
$\mathcal{X} \in \mathbb{R}^{T \times D}$	Time series with T time steps and D variates
$\mathcal{M} \in \{0, 1\}^{T \times D}$	Mask matrix for the time series
$\mathbf{X} \in \mathbb{R}^{L \times D}$	A lookback window of length L
$\mathbf{x}_t \in \mathbb{R}^D$	Observation at time step t
$\mathbf{M}^x \in \{0, 1\}^{L \times D}$	Mask matrix for a lookback window
$E^\tau \in \mathbb{R}^{L \times C}$	Timestamp embed. for a lookback window
$\mathbf{Y} \in \mathbb{R}^{H \times D}$	A forecasting window of length H
$\mathbf{M}^y \in \{0, 1\}^{H \times D}$	Mask matrix for a forecasting window

work designed to overcome the challenge of missing data. Table 1 summarizes the notations used in this paper.

3.1 Preliminaries

Let $\mathcal{X} = \{\mathbf{x}_1, \dots, \mathbf{x}_T\} \in \mathbb{R}^{T \times D}$ denote a multivariate time series with T time steps and D variates. As shown in Fig. 2, each observation $\mathbf{x}_t \in \mathbb{R}^D$ at time step t may contain missing values due to sensor malfunctions, communication failures and so on. We represent these missing patterns of the multivariate time series using a mask matrix $\mathcal{M} \in \{0, 1\}^{T \times D}$:

$$\mathbf{m}_{t,d} = \begin{cases} 1, & \text{if } \mathbf{x}_{t,d} \text{ is observed} \\ 0, & \text{otherwise.} \end{cases} \quad (1)$$

where $\mathbf{m}_{t,d}$ indicates the t -row, n -column element of \mathcal{M} . It has been demonstrated that incorporating the mask matrix to the training process is of great importance, as it allows

models to distinguish between actual zeros and missing values [14], [33]. Given a lookback window (a.k.a. historical observations) $\mathbf{X} = \mathcal{X}_{t-L+1:t} \in \mathbb{R}^{L \times D}$ of length L as well as its corresponding mask matrix $\mathbf{M}^x = \mathcal{M}_{t-L+1:t} \in \{0, 1\}^{L \times D}$, the goal of MTSF with missing values is to predict a forecasting window $\mathbf{Y} = \mathcal{X}_{t+1:t+H} \in \mathbb{R}^{H \times D}$ of length H , using a neural network $f_{\Theta} : (\mathbf{X}, \mathbf{M}^x) \mapsto \mathbf{Y}$, where Θ denotes the learnable parameters.

3.2 Overview

Unlike most previous approaches that adopt a sequential input-then-forecast paradigm, CoIFNet unifies imputation and forecasting in a single framework for achieving robust MTSF in the presence of missing values.

An overview of our proposed CoIFNet is illustrated in Fig. 3. Specifically, we first devise a *Reversal Observed-value Normalization (RevON)* module to reduce data distribution shifts across time steps within the input lookback window \mathbf{X} , yielding the normalized input $\tilde{\mathbf{X}} \in \mathbb{R}^{L \times D}$. Second, we concatenate $\tilde{\mathbf{X}} \in \mathbb{R}^{L \times D}$ with the mask matrix \mathbf{M}^x and timestamp embeddings $E^\tau \in \mathbb{R}^{L \times C}$ to produce $Z_{\text{in}} \in \mathbb{R}^{L \times (2D+C)}$. This composite input is processed by the *Cross-Timestep Fusion (CTF)* module to obtain timestep-attentive representations $Z_{\text{CTF}} \in \mathbb{R}^{H \times (2D+C)}$. Third, the *Cross-Variate Fusion (CVF)* module takes Z_{CTF} as input to obtain variate-attentive representations $Z_{\text{CVF}} \in \mathbb{R}^{H \times D}$. Fourth, Z_{CVF} are de-normalized in the original data space to obtain the imputed/reconstructed lookback window $\tilde{\mathbf{X}} \in \mathbb{R}^{L \times D}$ and the predicted forecasting window $\tilde{\mathbf{Y}} \in \mathbb{R}^{H \times D}$. Finally, an imputation loss \mathcal{L}_I together with a forecasting loss \mathcal{L}_F are respectively built on $(\tilde{\mathbf{X}}, \mathbf{X})$ and $(\tilde{\mathbf{Y}}, \mathbf{Y})$ to jointly update the network parameters.

3.3 Reversible Observed-value Normalization (RevON)

Real-world time series often exhibit non-stationarity, characterized by changes in statistical properties (such as mean and variance) across time steps. This phenomenon can lead to discrepancies across different time periods and affect a model's ability to generalize from past data to future events. Instance normalization has proven critically important for mitigating this issue. However, existing methods such as Reversible Instance Normalization (RevIN) [42], which use affine transformations to mitigate discrepancies across historical sequences, rely on complete time series to compute statistics such as mean and variance.

To tackle this limitation, we devise Reversible Observed-value Normalization (RevON), which calculates normalization statistics using (partially) observed time series values. Given the mask matrix $\mathbf{M}^x = \{\mathbf{m}_1, \dots, \mathbf{m}_L\}$ of a lookback window $\mathbf{X} = \{\mathbf{x}_1, \dots, \mathbf{x}_L\}$, RevON takes the form of

$$\begin{aligned} \mathbb{E}[\mathbf{X}] &= \frac{1}{\sum_{t=1}^L \mathbf{M}_t^x} \sum_{t=1}^L \mathbf{M}_t^x \mathbf{x}_t, \\ \text{Var}[\mathbf{X}] &= \frac{1}{\sum_{t=1}^L \mathbf{M}_t^x} \sum_{t=1}^L \mathbf{M}_t^x (\mathbf{M}_t^x - \mathbb{E}[\mathbf{X}])^2. \end{aligned} \quad (2)$$

Thus, the normalized representations can be expressed as

$$\tilde{\mathbf{X}} = \left(\gamma \odot \left(\frac{\mathbf{X} - \mathbb{E}[\mathbf{X}]}{\sqrt{\text{Var}[\mathbf{X}] + \epsilon}} \right) + \beta \right) \odot \mathbf{M}^x, \quad (3)$$

where γ and β are learnable weights and ϵ is a hyperparameter controlling stability.

3.4 Cross-Timestep Fusion (CTF)

Temporal context is critically important for processing incomplete time series, as it can compensate for the information distortion caused by missing values. Therefore, the Cross-Timestep Fusion (CTF) module of CoIFNet is first designed to fuse information along the timestep dimension to capture temporal dependencies within each variate of the multivariate time series.

Prior works have demonstrated the importance of leveraging timestamp information in time series to capture cyclical patterns [25], [43]. Motivated by this, we first extract the timestamp embeddings $E^\tau = \text{Embedding}(\tau)$ using the methodology introduced [25], and then we concatenate E^τ with the normalized time series data $\tilde{\mathbf{X}}$ and the corresponding mask matrix \mathbf{M}^x to obtain the input temporal representations:

$$Z_{\text{in}} = [\tilde{\mathbf{X}} \parallel \mathbf{M}^x \parallel E^\tau] \in \mathbb{R}^{L \times (2D+C)}, \quad (4)$$

where

$$E^\tau = [E_{\text{day}} \parallel E_{\text{hour}}] \in \mathbb{R}^{L \times C}, \quad (5)$$

$E_{\text{day}} \in \mathbb{R}^{L \times C_d}$ and $E_{\text{hour}} \in \mathbb{R}^{L \times C_h}$ denote day-of-week and hour-of-day timestamp embeddings respectively.

Given this composite input representation Z_{in} , the CTF module learns temporal dependencies along the time step dimension through an adaptive gating mechanism:

$$\begin{aligned} Z_d &= \sigma(W_\alpha Z_{\text{in}} + b_\alpha) \odot (W_d Z_{\text{in}} + b_d), \\ Z_{\text{CTF}} &= W_p \cdot \text{Dropout}(Z_d) + b_p, \end{aligned} \quad (6)$$

where $W_\alpha, W_d \in \mathbb{R}^{L \times h}$, $W_p \in \mathbb{R}^{h \times h}$ and $b_\alpha, b_d, b_p \in \mathbb{R}^h$ are learnable parameters, with h representing the hidden layer dimension. The function $\sigma(\cdot)$ denotes the sigmoid activation and \odot represents element-wise multiplication. The sigmoid gate $\sigma(W_\alpha Z_{\text{in}} + b_\alpha)$ produces values between 0 and 1, controlling how much information from each temporal feature is preserved. Intuitively, this selective attention mechanism enables the model to focus on learning patterns relevant to observed values while reducing the influence of uncertain or noisy features that may result from missing data.

3.5 Cross-Variate Fusion (CVF)

Subsequently, the CVF module models the temporal dependencies along the variate dimension of $Z_{\text{CTF}} \in \mathbb{R}^{h \times (2D+C)}$. Formally, CVF can be expressed as

$$\begin{aligned} Z'_d &= \sigma(W'_\alpha Z_{\text{CTF}} + b'_\alpha) \odot (W'_d Z_{\text{CTF}} + b'_d), \\ Z_{\text{CVF}} &= W'_p \cdot \text{Dropout}(Z'_d) + b'_p, \end{aligned} \quad (7)$$

where $W'_\alpha, W'_d \in \mathbb{R}^{(2D+C) \times D}$, $W'_p \in \mathbb{R}^{D \times D}$, and $b'_\alpha, b'_d, b'_p \in \mathbb{R}^D$ are learnable parameters. Similar to the CTF module, CVF employs a sigmoid-gated mechanism to adaptively focus on relevant cross-variate interactions while suppressing less informative ones. This adaptive approach is particularly beneficial when dealing with partially observed multivariate time series, as it helps mitigate the impact of missing values on cross-variate relationships.

Algorithm 1 Training pipeline of CoIFNet

Input: Multivariate time series \mathcal{X} , mask matrix \mathcal{M} , timestamp features \mathcal{T} , hyperparameter λ

Output: Trained model parameters Θ

- 1: Initialize model parameters Θ
- 2: **while** not converged **do**
- 3: Sample $(\mathbf{X}, \mathbf{Y}) \sim \mathcal{X}$, $(\mathbf{M}^x, \mathbf{M}^y) \sim \mathcal{M}$, $\tau \sim \mathcal{T}$
- 4: $\tilde{\mathbf{X}} \leftarrow \text{RevON}(\mathbf{X}, \mathbf{M}^x)$
- 5: $E^\tau \leftarrow \text{Embedding}(\tau)$
- 6: $Z_{\text{in}} \leftarrow [\tilde{\mathbf{X}} \parallel \mathbf{M}^x \parallel E^\tau]$
- 7: $Z_{\text{CTF}} \leftarrow \text{CTF}(Z_{\text{in}})$
- 8: $Z_{\text{CVF}} \leftarrow \text{CVF}(Z_{\text{CTF}})$
- 9: $[\tilde{\mathbf{X}}, \tilde{\mathbf{Y}}] \leftarrow \text{Projection}(Z_{\text{CVF}})$
- 10: $[\hat{\mathbf{X}}, \hat{\mathbf{Y}}] \leftarrow \text{De-Norm.}([\tilde{\mathbf{X}}, \tilde{\mathbf{Y}}])$
- 11: Calculate \mathcal{L}_I and \mathcal{L}_F
- 12: Update Θ by minimizing $\mathcal{L} = (1 - \lambda)\mathcal{L}_I + \lambda\mathcal{L}_F$
- 13: **end while**
- 14: **return** Θ

Next, we project Z_{CVF} to the original (low-dimensional) data space to simultaneously obtain the reconstructed historical values $\tilde{\mathbf{X}}$ and the predicted future values $\tilde{\mathbf{Y}}$:

$$[\tilde{\mathbf{X}}, \tilde{\mathbf{Y}}] = W_o Z_{\text{CVF}} + b_o, \quad (8)$$

where $W_o \in \mathbb{R}^{h \times (L+H)}$ and $b_o \in \mathbb{R}^{L+H}$ are learnable parameters, with L and H representing the historical and forecast horizon lengths respectively. Finally, we apply a de-normalization process of RevON to align the statistical information of $[\tilde{\mathbf{X}}, \tilde{\mathbf{Y}}]$ to the original data distribution:

$$[\hat{\mathbf{X}}, \hat{\mathbf{Y}}] = \sqrt{\text{Var}[\mathbf{X}] + \epsilon} \odot \left(\frac{[\tilde{\mathbf{X}}, \tilde{\mathbf{Y}}] - \beta}{\gamma} \right) + \mathbb{E}[\mathbf{X}], \quad (9)$$

where $\hat{\mathbf{X}} = \{\hat{x}_1, \dots, \hat{x}_L\}$, $\hat{\mathbf{Y}} = \{\hat{y}_1, \dots, \hat{y}_H\}$ and γ and β are the learnable parameters in Eq. 2.

3.6 Learning Objective

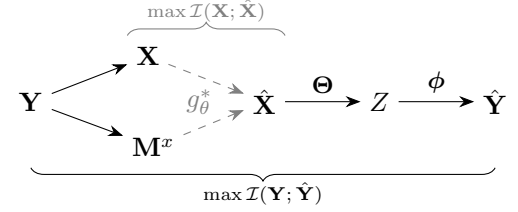
The overall learning objective of the proposed CoIFNet is defined as a weighted combination of the imputation loss \mathcal{L}_I and the prediction loss \mathcal{L}_F :

$$\mathcal{L} = (1 - \lambda)\mathcal{L}_I + \lambda\mathcal{L}_F, \quad (10)$$

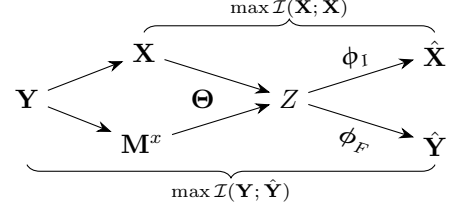
where $\lambda \in [0, 1]$ is a hyperparameter controlling the relative importance of the two losses:

$$\begin{aligned} \mathcal{L}_I &= \frac{\sum_t \mathbf{M}_t^x \cdot |\mathbf{X}_t - \hat{\mathbf{X}}_t|}{\sum_t \mathbf{M}_t^x}, \quad t = 1, \dots, L \\ \mathcal{L}_F &= \frac{\sum_h \mathbf{M}_h^y \cdot |\mathbf{Y}_h - \hat{\mathbf{Y}}_h|}{\sum_h \mathbf{M}_h^y}, \quad h = 1, \dots, H. \end{aligned} \quad (11)$$

In this way, CoIFNet integrates imputation and forecasting into a unified framework, enabling end-to-end learning of temporal dependencies from incomplete time series data. As a lightweight network architecture, CoIFNet ensures lower computational complexity and faster execution speeds (as demonstrated in Section 5.4), which makes it highly suitable for deployment in resource-constrained environments. The training pipeline for CoIFNet is detailed in **Algorithm 1**.



(a) Traditional impute-then-forecast approaches



(b) Our proposed CoIFNet framework

Fig. 4: Qualitative comparison of information flow between traditional impute-then-forecast approaches and our proposed CoIFNet framework. (a) The mask matrix \mathbf{M}^x used in the imputation stage becomes inaccessible during forecasting, breaking the Markov chain continuity from \mathbf{Y} to $\hat{\mathbf{Y}}$. **(b)** CoIFNet unifies imputation and forecasting in a single framework, enabling Markov chain continuity and preserving all information critical for accurate time series forecasting in the presence of missing data.

4 THEORETICAL ANALYSIS

In this section, we provide formal justifications grounded in the concept of *mutual information* [17], demonstrating how the CoIFNet learning objective enhances the performance bound for MTSF in the presence of missing data.

4.1 Information Loss in the Two-stage Pipeline

Traditional approaches to missing data in time series follow a two-stage pipeline: imputing missing values then performing forecasting on the imputed data. As depicted in Fig. 4(a), the mask matrix \mathbf{M}^x used in the imputation stage becomes inaccessible during forecasting, breaking the Markov chain continuity from \mathbf{Y} to $\hat{\mathbf{Y}}$. According to the Data Processing Inequality (DPI) [44] theory, we have:

$$\mathcal{I}(\mathbf{Y}; \mathbf{X}, \mathbf{M}^x) \geq \mathcal{I}(\mathbf{Y}; \hat{\mathbf{X}}). \quad (12)$$

where $\mathcal{I}(\cdot)$ denotes the amount of mutual information. The DPI Equation (12) holds with equality *only* if no information about \mathbf{Y} is lost during processing. However, the two-stage pipeline inherently causes information loss and results in a strict DPI inequality due to: 1) the imputation stage optimizes $\hat{\mathbf{X}}$ for reconstruction instead of forecasting, discarding a part of information critical for accurate forecasting [37], and 2) the mask matrix \mathbf{M}^x , which holds valuable forecasting signals, is discarded after imputation [45].

4.2 Information Preservation via Joint Optimization

Instead of following the restrictive path $(\mathbf{X}, \mathbf{M}^x) \xrightarrow{g_\theta^*} \hat{\mathbf{X}} \xrightarrow{f_{\Theta, \phi}} \hat{\mathbf{Y}}$, we propose to learn from $(\mathbf{X}, \mathbf{M}^x)$ and produce both $\hat{\mathbf{X}}$ and $\hat{\mathbf{Y}}$ simultaneously. This preserves access to all input

information throughout the learning process while maintaining the benefits of both imputation and forecasting objectives (as illustrated in Fig. 4(b)). To formalize this intuition, we relate mutual information to the Mean Absolute Error (MAE) loss. The choice of MAE is motivated by its inherent robustness, which makes it particularly well-suited for time series forecasting with missing data, as highlighted by [46]. This robustness stems from MAE's equivalence to maximizing likelihood under an assumption of Laplacian-distributed prediction errors, providing the theoretical foundation for our analysis. We employ a variational distribution $q(\mathbf{Y}|\hat{\mathbf{Y}})$ to approximate the true conditional probability $p(\mathbf{Y}|\hat{\mathbf{Y}})$, leading to the following proposition.

Proposition 1. *Under the assumption that prediction errors follow a Laplacian distribution, the mutual information $\mathcal{I}(\mathbf{Y}; \hat{\mathbf{Y}})$ between the ground truth values \mathbf{Y} and predictions $\hat{\mathbf{Y}}$ is lower-bounded by:*

$$\mathcal{I}(\mathbf{Y}; \hat{\mathbf{Y}}) \geq \mathcal{C} - \frac{1}{b} \mathbb{E} [\|\mathbf{Y} - \hat{\mathbf{Y}}\|_1],$$

where $\mathcal{C} = \mathcal{H}(\mathbf{Y}) - \log(2b)$, $b > 0$ is the scale parameter of the variational Laplacian distribution $q(\mathbf{Y}|\hat{\mathbf{Y}})$, and $\mathcal{H}(\mathbf{Y})$ is the entropy of \mathbf{Y} .

Proof: Denote the mutual information of the ground truth \mathbf{Y} and prediction $\hat{\mathbf{Y}}$ as:

$$\begin{aligned} \mathcal{I}(\mathbf{Y}; \hat{\mathbf{Y}}) &= \sum_{\mathbf{Y}, \hat{\mathbf{Y}}} p(\mathbf{Y}, \hat{\mathbf{Y}}) \log \frac{p(\mathbf{Y}, \hat{\mathbf{Y}})}{p(\mathbf{Y})p(\hat{\mathbf{Y}})} \\ &= \sum_{\mathbf{Y}, \hat{\mathbf{Y}}} p(\mathbf{Y}, \hat{\mathbf{Y}}) \log \frac{p(\mathbf{Y}, \hat{\mathbf{Y}})}{p(\hat{\mathbf{Y}})} \\ &\quad - \sum_{\mathbf{Y}, \hat{\mathbf{Y}}} p(\mathbf{Y}, \hat{\mathbf{Y}}) \log p(\mathbf{Y}) \\ &= \sum_{\mathbf{Y}, \hat{\mathbf{Y}}} p(\hat{\mathbf{Y}}) p(\mathbf{Y}|\hat{\mathbf{Y}}) \log p(\mathbf{Y}|\hat{\mathbf{Y}}) \\ &\quad - \sum_{\mathbf{Y}, \hat{\mathbf{Y}}} p(\mathbf{Y}, \hat{\mathbf{Y}}) \log p(\mathbf{Y}) \\ &= \mathcal{H}(\mathbf{Y}) - \mathcal{H}(\mathbf{Y}|\hat{\mathbf{Y}}) \\ &= \mathcal{H}(\mathbf{Y}) + \mathbb{E}_{\mathbf{Y}, \hat{\mathbf{Y}}} [\log p(\mathbf{Y}|\hat{\mathbf{Y}})] \end{aligned} \quad (13)$$

Since the true conditional distribution $p(\mathbf{Y}|\hat{\mathbf{Y}})$ is intractable, we introduce a variational distribution $q(\mathbf{Y}|\hat{\mathbf{Y}})$ to approximate it. The mutual information can then be expressed as:

$$\begin{aligned} \mathcal{I}(\mathbf{Y}; \hat{\mathbf{Y}}) &= \mathcal{H}(\mathbf{Y}) + \mathbb{E}_{\hat{\mathbf{Y}}} [\log q(\mathbf{Y}|\hat{\mathbf{Y}})] \\ &\quad + \mathbb{E}_{\hat{\mathbf{Y}}} [\mathcal{D}_{\text{KL}}(p(\mathbf{Y}|\hat{\mathbf{Y}}) \| q(\mathbf{Y}|\hat{\mathbf{Y}}))] \\ &\geq \mathcal{H}(\mathbf{Y}) + \mathbb{E}_{\mathbf{Y}, \hat{\mathbf{Y}}} [\log q(\mathbf{Y}|\hat{\mathbf{Y}})] \end{aligned} \quad (14)$$

The inequality holds due to the non-negativity of the KL divergence $\mathcal{D}_{\text{KL}}(p \| q)$. We assume $q(\mathbf{Y}|\hat{\mathbf{Y}})$ is a Laplacian distribution centered at $\hat{\mathbf{Y}}$ with scale $b > 0$, i.e.,

$$q(\mathbf{Y}|\hat{\mathbf{Y}}) = \frac{1}{2b} \exp \left(-\frac{\|\mathbf{Y} - \hat{\mathbf{Y}}\|_1}{b} \right). \quad (15)$$

Substituting the logarithm of Eq. (15) into the lower bound:

$$\begin{aligned} \mathcal{I}(\mathbf{Y}; \hat{\mathbf{Y}}) &\geq \mathcal{H}(\mathbf{Y}) + \mathbb{E} [\log q(\mathbf{Y}|\hat{\mathbf{Y}})] \\ &= \mathcal{H}(\mathbf{Y}) + \mathbb{E} \left[\log \left(\frac{1}{2b} \right) - \frac{\|\mathbf{Y} - \hat{\mathbf{Y}}\|_1}{b} \right] \\ &= \mathcal{H}(\mathbf{Y}) - \log(2b) - \frac{1}{b} \mathbb{E} [\|\mathbf{Y} - \hat{\mathbf{Y}}\|_1] \\ &= \mathcal{C} - \frac{1}{b} \mathbb{E} [\|\mathbf{Y} - \hat{\mathbf{Y}}\|_1] \end{aligned} \quad (16)$$

where $\mathcal{C} = \mathcal{H}(\mathbf{Y}) - \log(2b)$ is constant. Thus, minimizing MAE is tantamount to maximizing a variational lower bound on $\mathcal{I}(\mathbf{Y}; \hat{\mathbf{Y}})$ under these Laplacian assumptions. \square

Proposition 1 reveals that minimizing the MAE directly maximizes the mutual information between the predictions and the ground truth, leading to the following corollary:

Corollary 1. *The mutual information for the imputation task satisfies:*

$$\mathcal{I}(\mathbf{X}; \hat{\mathbf{X}}) \geq \mathcal{C}' - \frac{1}{b'} \mathbb{E} [\|\mathbf{X} - \hat{\mathbf{X}}\|_1],$$

where \mathcal{C}' and $b' > 0$ are corresponding constants for \mathbf{X}

This indicates that joint optimization of imputation and forecasting preserves information for the both tasks.

Proposition 2. *Let Z be an internal representation learned from input $(\mathbf{X}, \mathbf{M}^x)$ through joint optimization. The total mutual information between Z and all relevant variables is lower-bounded by:*

$$\begin{aligned} \mathcal{I}(\mathbf{X}; Z) + \mathcal{I}(\mathbf{Y}; Z) &\geq \mathcal{C}'' - \left(\frac{\mathbb{E} [\|\mathbf{Y} - \hat{\mathbf{Y}}\|_1]}{b} + \frac{\mathbb{E} [\|\mathbf{X} - \hat{\mathbf{X}}\|_1]}{b'} \right) \end{aligned}$$

where $\mathcal{C}'' = \mathcal{C} + \mathcal{C}'$ combines the entropy terms of the imputation and forecasting tasks.

Proof: We first bound the mutual information $\mathcal{I}(Z; \mathbf{X}, \mathbf{M}^x, \mathbf{Y})$ by decomposing it into components related to imputation and forecasting tasks. Since Z is learned to optimize both tasks, we have:

$$\mathcal{I}(\mathbf{X}, \mathbf{M}^x, \mathbf{Y}; Z) \geq \mathcal{I}(\mathbf{X}; Z) + \mathcal{I}(\mathbf{Y}; Z)$$

Thus,

$$\mathcal{I}(\mathbf{X}; Z) + \mathcal{I}(\mathbf{Y}; Z) \geq \mathcal{I}(\mathbf{X}; \hat{\mathbf{X}}) + \mathcal{I}(\mathbf{Y}; \hat{\mathbf{Y}})$$

According to Proposition 1 and Corollary 1, we have

$$\begin{aligned} \mathcal{I}(\hat{\mathbf{X}}; \mathbf{X}) + \mathcal{I}(\hat{\mathbf{Y}}; \mathbf{Y}) &\geq \left(\mathcal{H}(\mathbf{X}) - \log(2b') - \frac{1}{b'} \mathbb{E} [\|\mathbf{X} - \hat{\mathbf{X}}\|_1] \right) \\ &\quad + \left(\mathcal{H}(\mathbf{Y}) - \log(2b) - \frac{1}{b} \mathbb{E} [\|\mathbf{Y} - \hat{\mathbf{Y}}\|_1] \right) \\ &= \mathcal{C}'' - \left(\frac{\mathbb{E} [\|\mathbf{Y} - \hat{\mathbf{Y}}\|_1]}{b} + \frac{\mathbb{E} [\|\mathbf{X} - \hat{\mathbf{X}}\|_1]}{b'} \right) \end{aligned}$$

where $\mathcal{C}'' = \mathcal{H}(\mathbf{Y}) + \mathcal{H}(\mathbf{X}) - \log(2b) - \log(2b')$ and $b, b' > 0$ are constants. So, minimizing imputation and forecasting MAE errors jointly means maximizes the lower bound on

the mutual information captured by the representation Z . \square

The representation Z has direct access to both observed values and the mask matrix M^x , ensuring no predictive information is discarded. Our CoIFNet framework implements this principle through the composite loss $\mathcal{L} = (1 - \lambda)\mathcal{L}_I + \lambda\mathcal{L}_F$, where $\lambda \in [0, 1]$ balances the imputation loss \mathcal{L}_I and forecasting loss \mathcal{L}_F . This ensures that the gradients from both objectives directly impact the shared representation Z , thereby maximizing information preservation for robust and accurate time series forecasting.

4.3 Discussion on the Underlying Assumption

It is worth noting that our formal connection between the MAE loss and mutual information in *Proposition 1* is established under the assumption of a Laplacian distribution for the prediction errors. This choice is motivated by the direct correspondence between minimizing MAE and maximizing the variational lower bound on mutual information, a common approach in information-theoretic analyses of robust models. However, the core principle motivating our joint optimization framework is more general. A parallel argument can be formulated for other common loss-distribution pairs. For instance, minimizing the Mean Squared Error (MSE) loss is tantamount to maximizing the mutual information lower bound under a Gaussian error assumption. Thus, while our specific derivation focuses on the empirically robust MAE/Laplacian case, the fundamental theoretical advantage of our unified CoIFNet framework—preserving predictive information by avoiding the information bottleneck inherent in two-stage pipelines (as illustrated in Fig. 4)—holds more broadly. The joint learning objective encourages the model to retain all features from both the observed data and the mask matrix that are pertinent to both tasks, a principle that is not confined to a single choice of error distribution.

5 EXPERIMENTS

In this section, we conduct experiments on six real-world time series forecasting datasets under different missing-data patterns to evaluate the effectiveness and efficiency of our CoIFNet framework. We first compare the performance of CoIFNet with state-of-the-art approaches in handling diverse missing-data scenarios. Then, we perform ablation studies and case analysis to investigate the impacts of different model design decisions. The results under the point or block missing rate of 0.1 are provided at the end.

5.1 Experiment Settings

Datasets: We include 6 most commonly used time series forecasting datasets in our experiments. Table 2 provides basic statistics for these datasets.

- **Weather**¹: Meteorological data consisting of 21 indicators recorded at 10-minute intervals from 07/2020 to 07/2021.
- **Exchange Rate**: Daily exchange rates for 8 countries from 1990 to 2016.

1. <https://www.bgc-jena.mpg.de/wetter/>

TABLE 2: Detailed dataset descriptions.

Datasets	# Dims.	# Points	Interval	Information
ETTh1, ETTh2	7	17420	1 hour	Electricity
ETTm1, ETTm2	7	69680	15 mins	Electricity
Weather	21	36761	10 mins	Weather
Exchange	8	7588	1 day	Economy

TABLE 3: Hyperparameter setting in our experiments. We keep the hyperparameters consistent across all datasets and missing-data scenarios.

Hyperparameters	Values
Hidden size	256
Day-of-week embedding size	8
Hour-of-day embedding size	8
Dropout	0.1
Learning rate	0.001
λ (balance weight)	0.2
Batch size	512
Epochs	100

- **ETT (ETTh1, ETTh2, ETTm1, ETTm2)**²: Electricity transformer temperatures and power load features at 1-hour (ETTh1, ETTh2) and 15-minute (ETTm1, ETTm2) intervals.

Missing Patterns: We consider two missing patterns in our experiments.

- **Point Missing:** A certain rate of points in time series are randomly masked as missing values.
- **Block Missing:** A certain rate of blocks $B_{t,c} \in \mathbb{R}^{l_t \times l_c}$ in time series are randomly masked as missing data, where the maximum temporal length l_t and feature dimension l_c are set to 10 and 5, respectively.

Comparison Methods: To evaluate the effectiveness of our CoIFNet, we compare it with a wide spectrum of state-of-the-art approaches, including imputation-based methods, vanilla MTSF methods, and end-to-end methods. To ensure a fair comparison, we use mean imputation to initialize all missing values for the baseline methods.

- **Traditional MTSF Methods:** These methods apply masks in the loss function to reduce the impact of missing data on forecasting performance.
 - **STID [25]:** A spatial-temporal interaction decomposition model that captures complex interactions in multivariate time series data.
 - **DLinear [24]:** A linear forecasting model optimized for computational efficiency and scalability in handling large datasets.
 - **AGCRN [22]:** Combining graph convolutional networks with recurrent architectures to model spatio-temporal dynamics effectively.
 - **MTGNN [23]:** Leveraging graph neural networks to model multivariate time series, focusing on spatial correlations and temporal patterns.
 - **iTransformer [5]:** A transformer architecture based model that claims the capability to perform multiple tasks, including both imputa-

2. <https://github.com/zhouhaoyi/ETDataset>

tion and forecasting, thereby providing a versatile solution for time series analysis.

- **GPT4TS [29]:** A large-scale generative pre-trained transformer model that emphasizes its ability to handle a variety of tasks such as imputation and forecasting, highlighting its adaptability and robustness in complex time series scenarios.
- **Imputation-based Methods:** These methods treat the lookback sequence and forecast horizon as a unified sequence, with the entire forecast horizon set as missing during evaluation.
 - **BRITS [14]:** Utilizing bidirectional recurrent neural networks to impute missing values, thereby enhancing the model’s ability to learn temporal dependencies from incomplete data.
 - **SAITS [33]:** Employing self-attention mechanisms to reconstruct missing values, leveraging temporal context and observed patterns for imputation.
- **End-to-End Methods:**
 - **BiTGraph [16]:** The previous state-of-the-art end-to-end framework that jointly learns the temporal dependencies and spatial structure from time series with missing data.

Implementation Details: In our experiments, each model is trained using the historical lookback window of length $L = 96$ to predict the future forecasting window of length $H = 96$. Table 3 presents the hyperparameter setting in our experiments. Note that, we keep the hyperparameters consistent across all datasets and missing-data scenarios. In other words, there is no cherry-picking of parameters for each setting. Besides, the missing rates for the point/block missing pattern are set to $\{0.3, 0.6\}$. We employ early stopping with a patience of 10 epochs to prevent overfitting and select the model with the best validation performance. For each experiment, we conduct three independent runs with different random seeds and report the average MAE and MSE results. We have made our code publicly available at <https://github.com/KaiTang-eng/CoIFNet>.

5.2 Comparison with State-of-the-art

Table 4 and Table 5 report the forecasting results of CoIFNet and state-of-the-art methods on six real-world datasets at various point and block missing rates, respectively. As can be seen, our CoIFNet consistently outperforms all competitors under all missing-data scenarios, demonstrating its effectiveness and robustness. Concretely, from the results in Table 4, we see that CoIFNet outperforms the previous state-of-the-art method BiTGraph by 18.73% (19.36%) in MAE and 22.51% (24.40%) in MSE when the point missing rate is 0.3 (0.6). From the results in Table 5, we can observe that our CoIFNet outperforms BiTGraph by 20.98% (19.54%) in MAE and 25.51% (23.81%) in MSE when the block missing rate is 0.3 (0.6). The superior performance of our CoIFNet over other methods highlight CoIFNet’s superior capability in maintaining forecasting accuracy under severe missing

conditions. Notably, CoIFNet yields lower standard deviations (i.e., $\pm .00$) in both MAE and MSE compared to other methods, highlighting its superior stability and robustness.

Additionally, comparing the results of Table 4 and Table 5, we have the following observations. Firstly, time series with missing blocks pose greater challenges than those with missing points for all methods. This is likely because temporal dependencies are more severely disrupted when consecutive observations are missing. Secondly, traditional imputation-based approaches like BRITS and SAITS exhibit suboptimal performance in both scenarios, especially at higher missing rates. This can be attributed to their emphasis on reconstruction rather than forecasting, leading to a misalignment between training and evaluation objectives. Thirdly, transformer-based architectures (i.e., iTransformer, PatchTST) demonstrate competitive performance under the point missing pattern but exhibit significant degradation under the block missing pattern. This performance disparity likely stems from the inherent limitations of self-attention mechanisms: while they can effectively interpolate missing values through global context aggregation, their ability to interpolate missing blocks of time series is constrained. Finally, BiTGraph generally shows superior performance than other previous methods, which confirms the importance of explicitly modeling missing patterns when dealing with structured missing values. However, the superior performance of our CoIFNet over BiTGraph also reveal that BiTGraph’s effectiveness is limited by its over-dependence on local spatial correlations and insufficient modeling of cross-timestep and cross-variate interactions.

5.3 Ablation Studies

In this part, we perform ablation studies to scrutinize the effectiveness of the components of CoIFNet and the impact of other design choices on CoIFNet. We conduct experiments on two representative datasets ETTm2 and Weather.

Effectiveness of the Designed Components: We investigate the effectiveness of each key component in our proposed CoIFNet by individually removing or replacing elements and measuring the resulting performance. Table 6 presents the results over the two datasets under different missing-data scenarios, where “Baseline” indicates that we directly perform vanilla forecasting on incomplete time series data, and “w/o CTF/CVF” denotes the CTF/CVF component is replaced by a linear layer.

From the reported results in Table 6, we have the following observations. Firstly, removing each component of CoIFNet results in performance degradation, demonstrating the effectiveness of these components in enhancing overall performance. Secondly, from the results of ①②③, we observe that incorporating the mask matrix and timestamp embeddings with the input time series data brings performance gains. Possible reasons are as follows: 1) The mask matrix enables models to distinguish between actual zeros and missing values during training. 2) The timestamp information in time series helps the model capture cyclical patterns, which is critical for improving forecasting performance in the presence of missing data. Thirdly, from the results of ④⑤⑥, we see that both the CTF and CVF modules play important roles in performance enhancement.

TABLE 4: Comparison with state-of-the-arts on six real-world datasets under the **Point** missing rates of 0.3 and 0.6.

Point: $r = 0.3$														
Dataset Metric	ETTh1		ETTh2		ETTm1		ETTh2		Weather		Exchange Rate		AVG	
	MAE	MSE	MAE	MSE	MAE	MSE	MAE	MSE	MAE	MSE	MAE	MSE	MAE	MSE
BRITS	0.814 \pm .01	1.207 \pm .02	1.156 \pm .01	2.361 \pm .06	0.751 \pm .02	1.027 \pm .02	1.108 \pm .14	2.086 \pm .59	0.429 \pm .06	0.410 \pm .08	1.123 \pm .17	1.883 \pm .53	0.897 \pm .07	1.496 \pm .22
SAITS	0.848 \pm .00	1.271 \pm .01	1.188 \pm .01	2.454 \pm .02	0.790 \pm .00	1.098 \pm .01	1.356 \pm .00	3.120 \pm .01	0.590 \pm .00	0.615 \pm .00	1.400 \pm .04	2.934 \pm .12	1.029 \pm .01	1.915 \pm .03
STID	0.469 \pm .00	0.494 \pm .00	0.369 \pm .01	0.297 \pm .01	0.374 \pm .00	0.342 \pm .00	0.316 \pm .00	0.233 \pm .00	0.209 \pm .00	0.160 \pm .00	0.301 \pm .01	0.166 \pm .01	0.340 \pm .00	0.282 \pm .00
MTGNN	0.498 \pm .00	0.521 \pm .00	0.443 \pm .01	0.407 \pm .03	0.417 \pm .01	0.400 \pm .00	0.333 \pm .00	0.238 \pm .01	0.226 \pm .01	0.179 \pm .01	0.329 \pm .00	0.196 \pm .00	0.374 \pm .01	0.323 \pm .01
AGCRN	0.651 \pm .02	0.846 \pm .03	0.589 \pm .04	0.775 \pm .10	0.498 \pm .00	0.515 \pm .02	0.378 \pm .01	0.321 \pm .03	0.217 \pm .00	0.170 \pm .00	0.473 \pm .02	0.406 \pm .03	0.467 \pm .02	0.506 \pm .04
DLinear	0.463 \pm .00	0.490 \pm .00	0.365 \pm .00	0.287 \pm .00	0.387 \pm .00	0.369 \pm .00	0.313 \pm .00	0.226 \pm .00	0.261 \pm .00	0.212 \pm .00	0.267 \pm .00	0.130 \pm .00	0.343 \pm .00	0.286 \pm .00
PatchTST	0.475 \pm .01	0.500 \pm .01	0.369 \pm .00	0.300 \pm .01	0.386 \pm .00	0.366 \pm .00	0.307 \pm .01	0.224 \pm .01	0.238 \pm .00	0.190 \pm .00	0.259 \pm .00	0.128 \pm .01	0.339 \pm .00	0.285 \pm .01
iTransformer	0.465 \pm .00	0.488 \pm .00	0.362 \pm .00	0.288 \pm .00	0.382 \pm .00	0.356 \pm .00	0.308 \pm .00	0.222 \pm .00	0.233 \pm .00	0.185 \pm .00	0.276 \pm .01	0.140 \pm .01	0.338 \pm .00	0.280 \pm .00
GPT4TS	0.481 \pm .00	0.506 \pm .01	0.398 \pm .00	0.339 \pm .01	0.385 \pm .00	0.363 \pm .00	0.294 \pm .00	0.213 \pm .00	0.232 \pm .00	0.189 \pm .00	0.299 \pm .01	0.167 \pm .01	0.348 \pm .00	0.296 \pm .01
BiTGraph	0.496 \pm .01	0.520 \pm .01	0.408 \pm .01	0.364 \pm .03	0.411 \pm .00	0.391 \pm .00	0.323 \pm .01	0.230 \pm .01	0.222 \pm .00	0.174 \pm .00	0.320 \pm .02	0.188 \pm .03	0.363 \pm .01	0.311 \pm .01
CoIFNet	0.452 \pm .00	0.481 \pm .00	0.315 \pm .00	0.234 \pm .00	0.351 \pm .00	0.318 \pm .00	0.252 \pm .00	0.172 \pm .00	0.195 \pm .00	0.153 \pm .00	0.209 \pm .00	0.088 \pm .00	0.295 \pm .00	0.241 \pm .00

Point: $r = 0.6$														
Dataset Metric	ETTh1		ETTh2		ETTm1		ETTh2		Weather		Exchange Rate		AVG	
	MAE	MSE	MAE	MSE	MAE	MSE	MAE	MSE	MAE	MSE	MAE	MSE	MAE	MSE
BRITS	0.823 \pm .02	1.214 \pm .04	1.001 \pm .11	1.759 \pm .46	0.795 \pm .01	1.060 \pm .02	1.014 \pm .05	1.730 \pm .11	0.405 \pm .01	0.377 \pm .02	1.199 \pm .08	2.099 \pm .22	0.873 \pm .04	1.373 \pm .15
SAITS	0.842 \pm .01	1.272 \pm .01	1.187 \pm .01	2.455 \pm .03	0.787 \pm .00	1.090 \pm .01	1.356 \pm .00	3.118 \pm .01	0.598 \pm .00	0.624 \pm .00	1.400 \pm .04	2.938 \pm .15	1.028 \pm .01	1.916 \pm .04
STID	0.497 \pm .01	0.537 \pm .00	0.415 \pm .00	0.363 \pm .00	0.395 \pm .00	0.370 \pm .00	0.359 \pm .01	0.304 \pm .01	0.222 \pm .00	0.170 \pm .00	0.337 \pm .02	0.207 \pm .03	0.371 \pm .01	0.325 \pm .01
MTGNN	0.521 \pm .01	0.558 \pm .01	0.447 \pm .00	0.406 \pm .01	0.433 \pm .01	0.425 \pm .02	0.363 \pm .02	0.279 \pm .03	0.236 \pm .01	0.187 \pm .01	0.376 \pm .01	0.254 \pm .02	0.396 \pm .01	0.352 \pm .01
AGCRN	0.677 \pm .02	0.889 \pm .02	0.578 \pm .01	0.712 \pm .01	0.496 \pm .01	0.535 \pm .03	0.408 \pm .02	0.348 \pm .04	0.229 \pm .01	0.178 \pm .01	0.541 \pm .04	0.491 \pm .05	0.488 \pm .02	0.525 \pm .03
DLinear	0.500 \pm .00	0.542 \pm .00	0.403 \pm .00	0.339 \pm .00	0.424 \pm .00	0.421 \pm .00	0.355 \pm .00	0.274 \pm .01	0.281 \pm .00	0.224 \pm .00	0.306 \pm .01	0.167 \pm .01	0.378 \pm .00	0.328 \pm .00
PatchTST	0.501 \pm .00	0.538 \pm .01	0.372 \pm .01	0.304 \pm .02	0.419 \pm .01	0.414 \pm .01	0.315 \pm .00	0.234 \pm .00	0.250 \pm .00	0.203 \pm .00	0.274 \pm .01	0.145 \pm .01	0.355 \pm .01	0.306 \pm .01
iTransformer	0.491 \pm .00	0.523 \pm .00	0.398 \pm .00	0.335 \pm .00	0.410 \pm .00	0.393 \pm .00	0.352 \pm .00	0.270 \pm .00	0.234 \pm .00	0.189 \pm .00	0.312 \pm .01	0.175 \pm .01	0.366 \pm .00	0.314 \pm .00
GPT4TS	0.524 \pm .01	0.568 \pm .01	0.436 \pm .02	0.414 \pm .05	0.406 \pm .00	0.391 \pm .00	0.331 \pm .02	0.272 \pm .04	0.255 \pm .00	0.212 \pm .00	0.408 \pm .03	0.331 \pm .05	0.393 \pm .01	0.365 \pm .02
BiTGraph	0.515 \pm .01	0.548 \pm .01	0.444 \pm .01	0.419 \pm .04	0.421 \pm .00	0.408 \pm .01	0.339 \pm .01	0.256 \pm .02	0.226 \pm .00	0.179 \pm .01	0.319 \pm .00	0.184 \pm .00	0.377 \pm .01	0.332 \pm .01
CoIFNet	0.467 \pm .00	0.499 \pm .00	0.323 \pm .00	0.246 \pm .00	0.363 \pm .00	0.337 \pm .01	0.256 \pm .00	0.176 \pm .00	0.200 \pm .00	0.157 \pm .00	0.216 \pm .00	0.093 \pm .00	0.304 \pm .00	0.251 \pm .00

TABLE 5: Comparison with state-of-the-arts on six real-world datasets under the **Block** missing rates of 0.3 and 0.6.

Block: $r = 0.3$														
Dataset Metric	ETTh1		ETTh2		ETTm1		ETTh2		Weather		Exchange Rate		AVG	
	MAE	MSE	MAE	MSE	MAE	MSE	MAE	MSE	MAE	MSE	MAE	MSE	MAE	MSE
BRITS	0.794 \pm .02	1.173 \pm .05	1.115 \pm .08	2.152 \pm .28	0.757 \pm .01	1.034 \pm .03	1.231 \pm .04	2.550 \pm .28	0.422 \pm .08	0.402 \pm .10	1.074 \pm .05	1.690 \pm .15	0.899 \pm .05	1.500 \pm .15
SAITS	0.850 \pm .00	1.283 \pm .01	1.188 \pm .00	2.454 \pm .01	0.789 \pm .00	1.096 \pm .01	1.353 \pm .00	3.107 \pm .03	0.594 \pm .00	0.618 \pm .00	1.395 \pm .03	2.907 \pm .11	1.028 \pm .01	1.911 \pm .03
STID	0.494 \pm .01	0.539 \pm .02	0.441 \pm .01	0.436 \pm .03	0.391 \pm .00	0.372 \pm .01	0.361 \pm .02	0.319 \pm .03	0.220 \pm .00	0.169 \pm .00	0.340 \pm .00	0.223 \pm .00	0.375 \pm .01	0.343 \pm .01
MTGNN	0.518 \pm .01	0.559 \pm .01	0.486 \pm .00	0.486 \pm .02	0.432 \pm .00	0.423 \pm .00	0.349 \pm .00	0.258 \pm .00	0.231 \pm .00	0.183 \pm .00	0.390 \pm .02	0.281 \pm .04	0.401 \pm .01	0.365 \pm .01
AGCRN	0.660 \pm .01	0.867 \pm .02	0.604 \pm .02	0.828 \pm .04	0.515 \pm .01	0.563 \pm .02	0.434 \pm .04	0.417 \pm .07	0.238 \pm .00	0.187 \pm .01	0.535 \pm .01	0.505 \pm .01	0.497 \pm .02	0.561 \pm .03
DLinear	0.491 \pm .00	0.542 \pm .01	0.450 \pm .01	0.438 \pm .02	0.425 \pm .00	0.424 \pm .00	0.417 \pm .01	0.395 \pm .02	0.289 \pm .00	0.232 \pm .00	0.376 \pm .01	0.254 \pm .02	0.408 \pm .00	0.381 \pm .01
PatchTST	0.492 \pm .00	0.528 \pm .01	0.417 \pm .01	0.387 \pm .01	0.416 \pm .00	0.407 \pm .00	0.360 \pm .01	0.319 \pm .01	0.259 \pm .00	0.206 \pm .00	0.343 \pm .02	0.239 \pm .04	0.381 \pm .01	0.348 \pm .01
iTransformer	0.498 \pm .00	0.540 \pm .01	0.465 \pm .01	0.461 \pm .02	0.423 \pm .01	0.413 \pm .01	0.416 \pm .01	0.381 \pm .01	0.256 \pm .00	0.203 \pm .00	0.396 \pm .02	0.296 \pm .04	0.409 \pm .01	0.382 \pm .01
GPT4TS	0.496 \pm .00	0.544 \pm .01	0.480 \pm .02	0.514 \pm .05	0.407 \pm .00	0.395 \pm .00	0.390 \pm .01	0.400 \pm .02	0.254 \pm .00	0.204 \pm .00	0.359 \pm .01	0.275 \pm .01	0.398 \pm .01	0.389 \pm .02
BiTGraph	0.519 \pm .01	0.558 \pm .01	0.430 \pm .01	0.384 \pm .02	0.420 \pm .00	0.408 \pm .00	0.336 \pm .02	0.248 \pm .02	0.229 \pm .00	0.181 \pm .01	0.381 \pm .04	0.266 \pm .07	0.386 \pm .01	0.341 \pm .02
CoIFNet	0.467 \pm .00	0.508 \pm .01	0.319 \pm .00	0.240 \pm .00	0.369 \pm .00	0.343 \pm .00	0.257 \pm .00	0.179 \pm .00	0.201 \pm .00	0.158 \pm .00	0.218 \pm .00	0.097 \pm .00	0.305 \pm .00	0.254 \pm .00

Block: $r = 0.6$														
Dataset Metric	ETTh1		ETTh2		ETTm1		ETTh2		Weather		Exchange Rate		AVG	
	MAE	MSE	MAE	MSE	MAE	MSE	MAE	MSE	MAE	MSE	MAE	MSE	MAE	MSE
BRITS	0.796 \pm .04	1.172 \pm .07	1.031 \pm .02	1.813 \pm .13	0.774 \pm .03	1.042 \pm .04	1.199 \pm .03	2.359 \pm .25	0.386 \pm .04	0.348 \pm .04	1.077 \pm .09	1.728 \pm .29	0.877 \pm .04	1.410 \pm .14
SAITS	0.844 \pm .00	1.265 \pm .00	1.183 \pm .01	2.436 \pm .03	0.788 \pm .00	1.097 \pm .00	1.362 \pm .00	3.145 \pm .01	0.600 \pm .00	0.628 \pm .00	1.399 \pm .04	2.922 \pm .13	2.398 \pm .51	3.233 \pm .53
STID	0.539 \pm .00	0.612 \pm .01	0.488 \pm .01	0.517 \pm .03	0.419 \pm .00	0.407 \pm .01	0.389 \pm .01	0.354 \pm .02	0.234 \pm .00	0.181 \pm .00	0.400 \pm .02	0.307 \pm .03	0.412 \pm .01	0.396 \pm .02
MTGNN	0.552 \pm .01	0.625 \pm .02	0.522 \pm .01	0.562 \pm .02	0.471 \pm .03	0.485 \pm .05	0.383 \pm .01	0.307 \pm .01	0.242 \pm .00	0.192 \pm .00	0.434 \pm .04	0.346 \pm .08	0.434 \pm .02	0.420 \pm .03
AGCRN	0.727 \pm .06	0.970 \pm .09	0.651 \pm .03	0.922 \pm .05	0.546 \pm .02	0.598 \pm .04	0.478 \pm .02	0.458 \pm .03	0.250 \pm .00	0.197 \pm .00	0.598 \pm .02	0.604 \pm .03	0.542 \pm .03	0.625 \pm .04
DLinear	0.549 \pm .00	0.643 \pm .01	0.524 \pm .01	0.573 \pm .01	0.478 \pm .00	0.508 \pm .01	0.506 \pm .00	0.545 \pm .01	0.314 \pm .00	0.253 \pm .00	0.450 \pm .02	0.363 \pm .04	0.470 \pm .01	0.481 \pm .01
PatchTST	0.537 \pm .00	0.605 \pm .02	0.391 \pm .01	0.328 \pm .02	0.467 \pm .00	0.473 \pm .01	0.331 \pm .00	0.259 \pm .00	0.270 \pm .00	0.219 \pm .00	0.384 \pm .02	0.311 \pm .04	0.397 \pm .01	0.366 \pm .01
iTransformer	0.543 \pm .00	0.621 \pm .01	0.527 \pm .01	0.580 \pm .03	0.460 \pm .00	0.472 \pm .00	0.383 \pm .00	0.320 \pm .01	0.249 \pm .00	0.204 \pm .00	0.432 \pm .03	0.360 \pm .05	0.432 \pm .01	0.426 \pm .02
GPT4TS	0.579 \pm .01	0.661 \pm .02	0.453 \pm .00	0.425 \pm .01	0.477 \pm .01	0.480 \pm .01	0.375 \pm .01	0.318 \pm .02	0.277 \pm .00	0.236 \pm .01	0.513 \pm .02	0.522 \pm .04	0.446 \pm .01	0.441 \pm .02
BiTGraph	0.543 \pm .02	0.608 \pm .03	0.448 \pm .01	0.417 \pm .01	0.442 \pm .01	0.439 \pm .02	0.337 \pm .01	0.249 \pm .02	0.234 \pm .00	0.186 \pm .00	0.359 \pm .02	0.243 \pm .04	0.394 \pm .01	0.357 \pm .02
CoIFNet	0.490 \pm .00	0.552 \pm .01	0.330 \pm .00	0.253 \pm .00	0.389 \pm .01	0.377 \pm .02	0.261 \pm .00	0.184 \pm .00	0.207 \pm .00	0.163 \pm .00	0.225 \pm .00	0.101 \pm .00	0.317 \pm .00	0.272 \pm .00

TABLE 6: Ablation study of the devised components of CoIFNet on the ETTm2 and Weather datasets at the point/block missing rates of 0.3 and 0.6. “w/o CTF/CVF” indicates the CTF/CVF component is replaced by a linear layer.

Setting		ETTm2				Weather			
		$r = 0.3$		$r = 0.6$		$r = 0.3$		$r = 0.6$	
		MAE	MSE	MAE	MSE	MAE	MSE	MAE	MSE
Point	CoIFNet	0.252\pm.00	0.172\pm.00	0.258\pm.00	0.179\pm.00	0.200\pm.00	0.157\pm.00	0.204\pm.00	0.161\pm.00
	① w/o M^x	0.254 \pm .00	0.174 \pm .00	0.260 \pm .00	0.181 \pm .00	0.200 \pm .00	0.157 \pm .00	0.206 \pm .00	0.163 \pm .00
	② w/o E_τ	0.253 \pm .00	0.173 \pm .00	0.262 \pm .00	0.183 \pm .00	0.203 \pm .00	0.159 \pm .00	0.208 \pm .00	0.164 \pm .00
	③ w/o M^x & E_τ	0.256 \pm .00	0.175 \pm .00	0.265 \pm .00	0.186 \pm .00	0.201 \pm .00	0.158 \pm .00	0.209 \pm .00	0.164 \pm .00
	④ w/o CTF	0.260 \pm .00	0.183 \pm .00	0.266 \pm .00	0.190 \pm .00	0.204 \pm .00	0.160 \pm .00	0.210 \pm .00	0.166 \pm .00
	⑤ w/o CVF	0.256 \pm .00	0.176 \pm .00	0.264 \pm .00	0.185 \pm .00	0.210 \pm .00	0.169 \pm .01	0.214 \pm .00	0.169 \pm .00
	⑥ w/o CTF & CVF	0.264 \pm .00	0.187 \pm .00	0.271 \pm .00	0.194 \pm .00	0.233 \pm .00	0.197 \pm .00	0.236 \pm .00	0.198 \pm .00
	⑦ w/o RevON	0.374 \pm .04	0.389 \pm .11	0.403 \pm .06	0.445 \pm .21	0.206 \pm .01	0.156 \pm .01	0.213 \pm .00	0.161 \pm .00
	⑧ Replace RevON by RevIN [42]	0.369 \pm .01	0.316 \pm .02	0.473 \pm .04	0.514 \pm .09	0.217 \pm .00	0.163 \pm .00	0.242 \pm .00	0.189 \pm .00
	⑨ Predict \hat{Y} only, rather than $[\hat{X}, \hat{Y}]$	0.263 \pm .00	0.189 \pm .00	0.271 \pm .00	0.200 \pm .00	0.212 \pm .01	0.169 \pm .00	0.218 \pm .01	0.174 \pm .01
Block	CoIFNet	0.258\pm.00	0.179\pm.00	0.263\pm.00	0.186\pm.00	0.203\pm.00	0.159\pm.00	0.213\pm.00	0.168\pm.00
	① w/o M^x	0.262 \pm .00	0.185 \pm .00	0.267 \pm .00	0.191 \pm .00	0.207 \pm .00	0.163 \pm .00	0.217 \pm .00	0.173 \pm .00
	② w/o E_τ	0.261 \pm .00	0.182 \pm .00	0.269 \pm .00	0.192 \pm .00	0.208 \pm .00	0.163 \pm .00	0.218 \pm .00	0.173 \pm .00
	③ w/o M^x & E_τ	0.263 \pm .00	0.184 \pm .00	0.271 \pm .00	0.195 \pm .00	0.210 \pm .00	0.163 \pm .00	0.217 \pm .00	0.171 \pm .00
	④ w/o CTF	0.265 \pm .00	0.190 \pm .01	0.268 \pm .00	0.191 \pm .00	0.212 \pm .00	0.167 \pm .00	0.221 \pm .00	0.177 \pm .00
	⑤ w/o CVF	0.263 \pm .00	0.186 \pm .00	0.270 \pm .00	0.194 \pm .00	0.209 \pm .00	0.164 \pm .00	0.219 \pm .00	0.173 \pm .00
	⑥ w/o CTF & CVF	0.268 \pm .00	0.193 \pm .00	0.277 \pm .00	0.201 \pm .00	0.236 \pm .00	0.196 \pm .00	0.240 \pm .00	0.200 \pm .00
	⑦ w/o RevON	0.405 \pm .06	0.485 \pm .20	0.441 \pm .02	0.471 \pm .06	0.220 \pm .01	0.168 \pm .00	0.224 \pm .00	0.173 \pm .01
	⑧ Replace RevON by RevIN [42]	0.372 \pm .01	0.334 \pm .01	0.498 \pm .03	0.567 \pm .06	0.227 \pm .00	0.168 \pm .00	0.240 \pm .00	0.181 \pm .00
	⑨ Predict \hat{Y} only, rather than $[\hat{X}, \hat{Y}]$	0.269 \pm .00	0.196 \pm .00	0.271 \pm .00	0.196 \pm .00	0.224 \pm .01	0.178 \pm .01	0.227 \pm .01	0.182 \pm .01

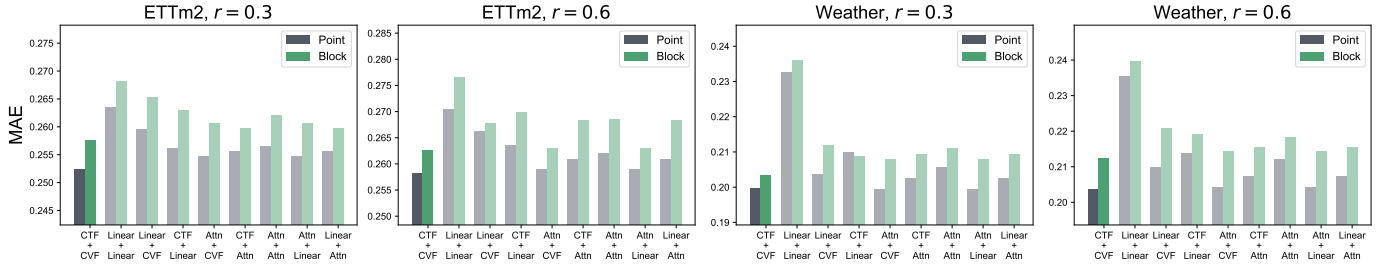


Fig. 5: Ablation study of the CTF and CVF modules on ETTm2 and Weather datasets across diverse missing-data scenarios.

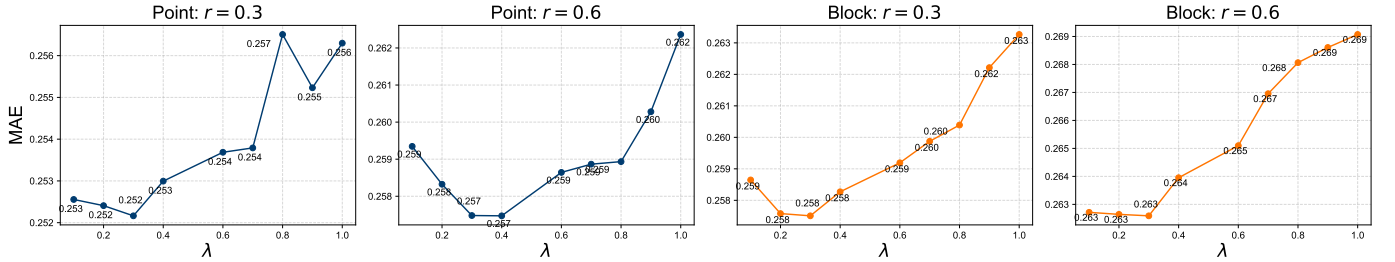


Fig. 6: Ablation study of the balance parameter λ on the ETTm2 dataset across diverse missing-data scenarios.

to CTF+CVF in the point missing pattern but it exhibits significant performance degradation in the block missing pattern, which highlights the effectiveness and efficiency of our proposed CoIFNet framework.

Impact of the Balance Weight λ . In the proposed CoIFNet, we employ the balance weight λ to control the relative importance of the imputation and forecasting losses. It is necessary to investigate the impact of λ on the performance of CoIFNet. To this end, we set λ to the values of $\{0.1, 0.2, \dots, 1.0\}$, and report the average testing results on the 6 datasets in Fig. 6. Overall, the performance of CoIFNet gradually increases as the λ value grows from 0.1 to 0.3, after which the performance of DePT gradually decreases and reaches the lowest value when $\lambda = 1.0$. In particular, when $\lambda = 0.3$ CoIFNet establishes the best performance across all those settings. What is noteworthy

is that when $\lambda = 1.0$, i.e., only the forecasting loss is used for training, the performance of CoIFNet sharply decreases, which suggests that joint optimization of imputation and forecasting objectives is of great importance for achieving better MTSF performance in the presence of missing values.

5.4 Computational Efficiency Analysis

Beyond forecasting accuracy, computational efficiency plays a crucial role in practical applications of time series models. We conduct a comprehensive efficiency analysis comparing CoIFNet with mainstream baselines in terms of model parameters and training time. The results are summarized in Fig. 7. As demonstrated, the efficiency advantages of CoIFNet manifest through three key aspects. Firstly, compared to BiTGraph, the previous state-of-the-art model

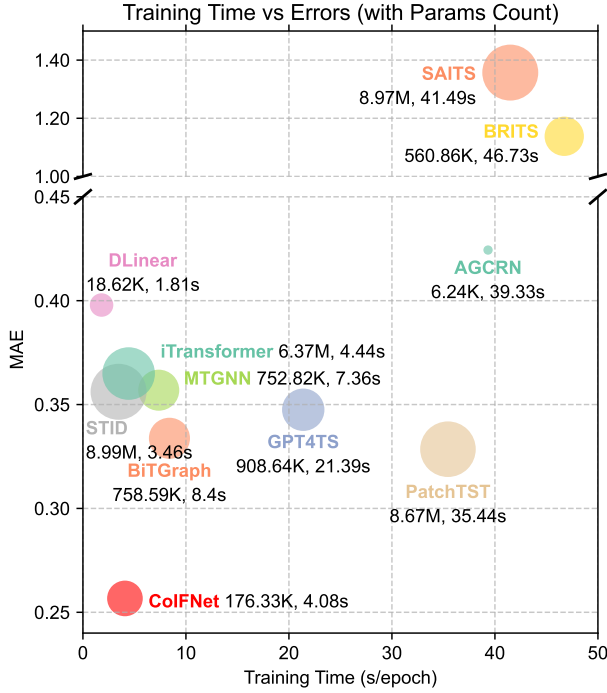


Fig. 7: Comparison of forecasting performance and computational efficiency for different methods on the ETTm2 dataset, under the block missing rate of 0.3.

for MTSF with missing values, CoIFNet achieves a **4.3×** improvement in memory efficiency and a **2.1×** gain in time efficiency. This efficiency stems from our carefully designed CTF and CVF module, which captures temporal dependencies through lightweight linear operations rather than quadratic-complexity attention mechanisms. Secondly, CoIFNet demonstrates significant computational efficiency advantages over Transformer-based architectures such as PatchTST, iTransformer, and GPT4TS. Although these models achieve improved predictive performance by leveraging self-attention mechanisms, their reliance on such operations results in substantial computational overhead. Thirdly, even compared to Linear-based models like STID, CoIFNet demonstrates comparable or superior computational efficiency. The main reason is that these rivals require more computational resources due to their relying on complex temporal dependence modeling modules. The lightweight architecture enables faster training and inference while maintaining robust performance across various missing patterns and missing rates. Those advantages render CoIFNet especially suitable for real-world deployments where both computational efficiency and forecasting accuracy are critical considerations.

5.5 Case Study

To provide deeper insights into model behavior, we conduct detailed case studies on the ETTm2 dataset under different missing scenarios. Fig. 8 presents the forecasting results of our proposed CoIFNet and three representative paradigms: BiTGraph, iTransformer, and BRITS. At a point missing rate of 0.3, we observe that while iTransformer captures the general trend of the time series, it struggles

to accurately predict the magnitude of peaks and troughs. BiTGraph demonstrates improved performance over iTransformer, confirming the value of explicitly modeling missing patterns. However, CoIFNet achieves the closest alignment with the ground truth, particularly in capturing the amplitude variations and temporal dynamics. BRITS, despite being designed for handling missing values, shows significant deviations from the ground truth, indicating that imputation-focused approaches without explicit forecasting optimization fail to adapt well to the forecasting task. As the missing rate increases to 0.6, the performance gap between different models widens. BRITS exhibits substantial prediction errors, iTransformer maintains reasonable trend prediction but misses important fluctuations in the time series. BiTGraph performs better than iTransformer, demonstrating the importance of specialized modeling for missing values scenarios. CoIFNet continues to provide the most accurate forecasts, with predictions that closely follow the ground truth curve even under this challenging high-missing-rate condition. At a block missing rate of 0.3, BRITS and iTransformer struggle significantly, failing to capture the temporal dynamics after extended missing segments. BiTGraph shows improved performance but still exhibits noticeable deviations from the ground truth. CoIFNet maintains superior prediction accuracy, effectively reconstructing the underlying patterns despite the presence of large missing blocks in the input data. As the missing rate increases to 0.6, the performance difference becomes most pronounced. BRITS produces forecasts that bear little resemblance to the actual time series, while iTransformer captures only the most basic trend. BiTGraph manages to approximate some features of the time series but misses critical temporal transitions. In contrast, CoIFNet continues to generate forecasts that closely align with the ground truth, demonstrating CoIFNet’s robustness against missing values.

5.6 Additional Results

Table 7 compares the time series forecasting performance of our CoIFNet approach with state-of-the-art methods on six real-world datasets, at a point/block missing rate of 0.1. As can be observed, CoIFNet achieves the best or comparable results across the six datasets demonstrating its effectiveness and robustness. On average, CoIFNet outperforms the previous state-of-the-art method BiTGraph by **15.56%** (**17.36%**) in MAE and **17.96%** (**21.36%**) in MSE when the point (block) missing rate is 0.1.

6 CONCLUSION

In this work, we propose CoIFNet, a unified and end-to-end framework for achieving robust multivariate time series forecasting (MTSF) in the presence of missing values. CoIFNet integrates the observed values, mask matrix, and timestamp embeddings, and processes them through sequential Cross-Timestep Fusion (CTF) and Cross-Variate Fusion (CVF) modules to capture temporal dependencies resilient to incomplete observations. We further provide theoretical justifications based on mutual information, proving the superiority of our one-stage CoIFNet framework over traditional two-stage approaches for handling missing values in time series forecasting. Extensive experiments on six

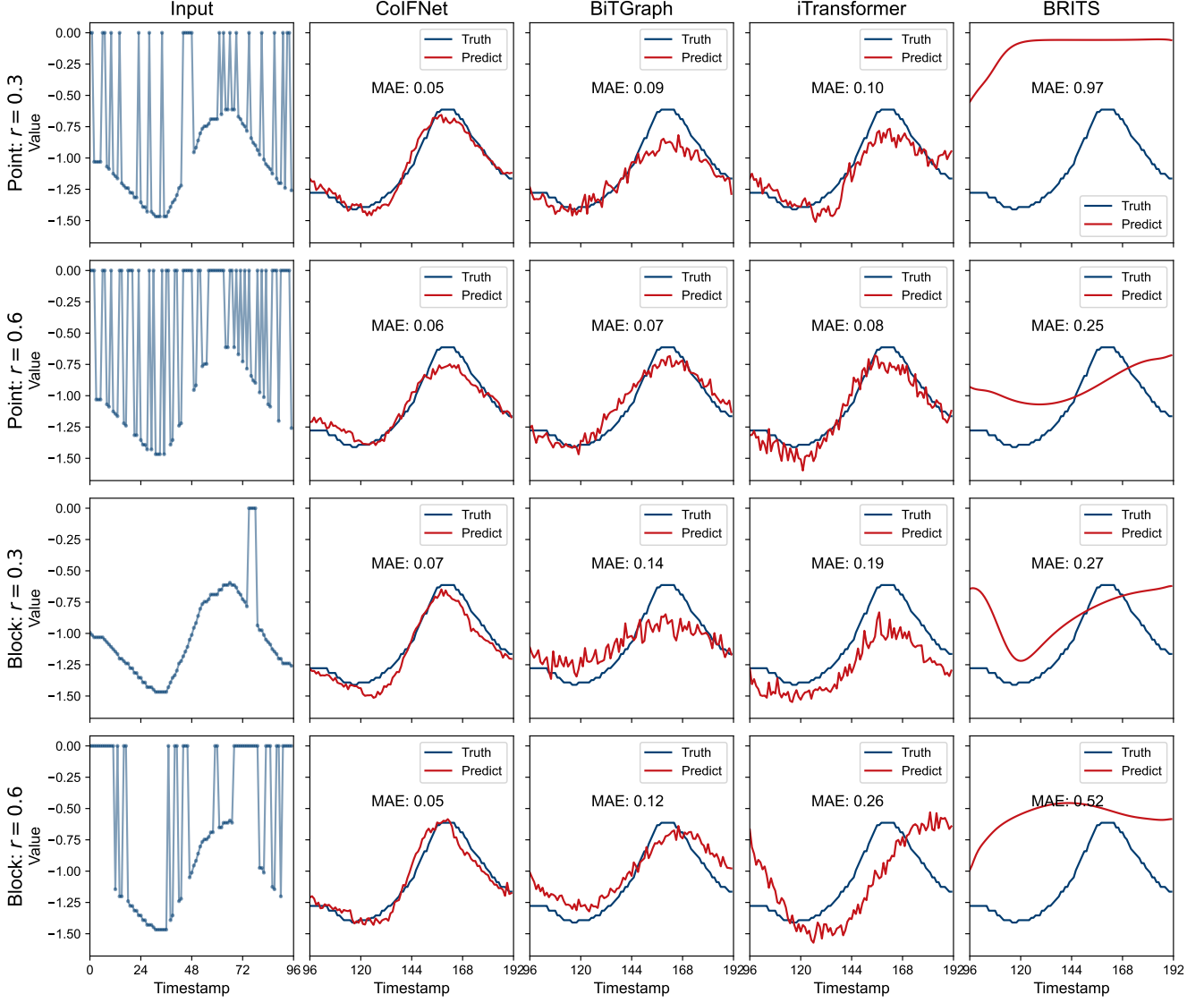


Fig. 8: Forecasting curves of BitGraph, iTransformer, BRITS and our CoIFNet on the ETTm2 dataset.

TABLE 7: Comparison with state-of-the-arts on six real-world datasets under the Point/Block missing rate of 0.1.

Point, $r = 0.1$														
Dataset	ETTh1		ETTh2		ETTm1		ETTm2		Weather		Exchange Rate		AVG	
Metric	MAE	MSE	MAE	MSE	MAE	MSE	MAE	MSE	MAE	MSE	MAE	MSE	MAE	MSE
BRITS	0.811 \pm .01	1.203 \pm .02	1.169 \pm .04	2.364 \pm .08	0.779 \pm .03	1.070 \pm .02	1.168 \pm .11	2.276 \pm .49	0.476 \pm .07	0.472 \pm .09	1.367 \pm .03	2.776 \pm .10	0.962 \pm .05	1.693 \pm .13
SAITS	0.841 \pm .00	1.268 \pm .00	1.187 \pm .01	2.437 \pm .03	0.789 \pm .00	1.097 \pm .01	1.353 \pm .00	3.108 \pm .02	0.587 \pm .00	0.611 \pm .00	1.397 \pm .04	2.916 \pm .13	1.029 \pm .01	1.906 \pm .03
STID	0.450 \pm .00	0.475 \pm .00	0.338 \pm .00	0.258 \pm .00	0.360 \pm .00	0.330 \pm .00	0.280 \pm .00	0.193 \pm .00	0.204 \pm .00	0.158 \pm .00	0.262 \pm .02	0.128 \pm .02	0.316 \pm .00	0.257 \pm .00
MTGNN	0.491 \pm .01	0.514 \pm .01	0.438 \pm .01	0.395 \pm .04	0.406 \pm .01	0.385 \pm .01	0.319 \pm .01	0.228 \pm .01	0.222 \pm .00	0.174 \pm .00	0.315 \pm .01	0.178 \pm .01	0.365 \pm .01	0.312 \pm .02
AGCRN	0.660 \pm .03	0.851 \pm .04	0.592 \pm .01	0.770 \pm .04	0.492 \pm .01	0.498 \pm .02	0.350 \pm .01	0.277 \pm .01	0.218 \pm .01	0.171 \pm .01	0.424 \pm .03	0.325 \pm .05	0.456 \pm .02	0.482 \pm .03
DLinear	0.445 \pm .00	0.469 \pm .00	0.338 \pm .00	0.256 \pm .00	0.365 \pm .00	0.346 \pm .00	0.288 \pm .00	0.203 \pm .00	0.247 \pm .00	0.207 \pm .00	0.233 \pm .00	0.101 \pm .00	0.319 \pm .00	0.264 \pm .00
PatchTST	0.454 \pm .00	0.476 \pm .00	0.333 \pm .00	0.257 \pm .00	0.363 \pm .00	0.342 \pm .00	0.276 \pm .00	0.196 \pm .00	0.222 \pm .00	0.181 \pm .00	0.229 \pm .01	0.100 \pm .01	0.313 \pm .00	0.259 \pm .00
iTransformer	0.470 \pm .00	0.488 \pm .01	0.368 \pm .00	0.296 \pm .01	0.384 \pm .00	0.349 \pm .00	0.301 \pm .00	0.218 \pm .00	0.236 \pm .00	0.183 \pm .00	0.287 \pm .00	0.163 \pm .01	0.341 \pm .00	0.283 \pm .00
GPT4TS	0.448 \pm .00	0.475 \pm .01	0.351 \pm .01	0.274 \pm .01	0.362 \pm .00	0.340 \pm .00	0.278 \pm .00	0.197 \pm .00	0.228 \pm .00	0.188 \pm .00	0.234 \pm .01	0.104 \pm .00	0.317 \pm .00	0.263 \pm .00
BitGraph	0.485 \pm .00	0.507 \pm .00	0.386 \pm .01	0.313 \pm .01	0.404 \pm .01	0.381 \pm .00	0.289 \pm .01	0.194 \pm .01	0.209 \pm .00	0.163 \pm .00	0.311 \pm .01	0.171 \pm .01	0.347 \pm .01	0.288 \pm .01
CoIFNet	0.445 \pm .00	0.471 \pm .00	0.313 \pm .00	0.231 \pm .00	0.346 \pm .00	0.313 \pm .00	0.249 \pm .00	0.169 \pm .00	0.198 \pm .00	0.156 \pm .00	0.206 \pm .00	0.088 \pm .00	0.293 \pm .00	0.238 \pm .00
Block, $r = 0.1$														
Dataset	ETTh1		ETTh2		ETTm1		ETTm2		Weather		Exchange Rate		AVG	
Metric	MAE	MSE	MAE	MSE	MAE	MSE	MAE	MSE	MAE	MSE	MAE	MSE	MAE	MSE
BRITS	0.802 \pm .01	1.185 \pm .03	1.076 \pm .10	2.025 \pm .41	0.780 \pm .02	1.067 \pm .03	1.246 \pm .05	2.632 \pm .26	0.426 \pm .01	0.400 \pm .01	1.235 \pm .11	2.202 \pm .36	0.928 \pm .05	1.585 \pm .18
SAITS	0.847 \pm .00	1.275 \pm .00	1.194 \pm .00	2.484 \pm .01	0.792 \pm .00	1.105 \pm .00	1.352 \pm .01	3.112 \pm .03	0.589 \pm .00	0.613 \pm .00	1.397 \pm .04	2.919 \pm .14	1.029 \pm .01	1.918 \pm .03
STID	0.462 \pm .00	0.485 \pm .01	0.368 \pm .01	0.310 \pm .01	0.373 \pm .01	0.347 \pm .00	0.310 \pm .00	0.243 \pm .01	0.207 \pm .00	0.162 \pm .00	0.280 \pm .01	0.161 \pm .01	0.334 \pm .01	0.285 \pm .01
MTGNN	0.497 \pm .00	0.518 \pm .00	0.440 \pm .03	0.415 \pm .05	0.419 \pm .00	0.407 \pm .01	0.336 \pm .01	0.245 \pm .00	0.219 \pm .00	0.171 \pm .00	0.354 \pm .01	0.238 \pm .02	0.378 \pm .01	0.332 \pm .01
AGCRN	0.648 \pm .01	0.826 \pm .01	0.635 \pm .03	0.876 \pm .07	0.509 \pm .02	0.522 \pm .03	0.430 \pm .05	0.438 \pm .12	0.222 \pm .00	0.174 \pm .00	0.473 \pm .02	0.396 \pm .04	0.486 \pm .02	0.539 \pm .05
DLinear	0.450 \pm .00	0.478 \pm .00	0.371 \pm .00	0.314 \pm .00	0.381 \pm .00	0.372 \pm .00	0.331 \pm .01	0.278 \pm .01	0.257 \pm .00	0.218 \pm .00	0.285 \pm .01	0.170 \pm .01	0.346 \pm .00	0.305 \pm .00
PatchTST	0.459 \pm .00	0.486 \pm .00	0.349 \pm .00	0.280 \pm .01	0.378 \pm .00	0.367 \pm .00	0.289 \pm .00	0.220 \pm .00	0.233 \pm .00	0.192 \pm .00	0.250 \pm .02	0.271 \pm .24	0.326 \pm .01	0.303 \pm .04
iTransformer	0.474 \pm .00	0.494 \pm .00	0.411 \pm .00	0.372 \pm .00	0.404 \pm .01	0.386 \pm .02	0.348 \pm .01	0.281 \pm .02	0.242 \pm .00	0.187 \pm .00	0.327 \pm .00	0.228 \pm .01	0.368 \pm .00	0.325 \pm .01
GPT4TS	0.451 \pm .00	0.482 \pm .00	0.368 \pm .00	0.314 \pm .01	0.372 \pm .00	0.361 \pm .00	0.297 \pm .01	0.234 \pm .01	0.231 \pm .00	0.192 \pm .00	0.252 \pm .00	0.136 \pm .01	0.329 \pm .00	0.286 \pm .00
BitGraph	0.498 \pm .01	0.520 \pm .01	0.414 \pm .04	0.359 \pm .05	0.413 \pm .01	0.394 \pm .00	0.312 \pm .01	0.217 \pm .01	0.215 \pm .00	0.167 \pm .00	0.323 \pm .01	0.199 \pm .01	0.362 \pm .01	0.309 \pm .02
CoIFNet	0.452 \pm .00	0.480 \pm .00	0.315 \pm .00	0.235 \pm .00	0.353 \pm .00	0.323 \pm .00	0.252 \pm .00	0.173 \pm .00	0.200 \pm .00	0.158 \pm .00	0.209 \pm .00	0.089 \pm .00	0.297 \pm .00	0.243 \pm .00

real-world datasets demonstrate the effectiveness and computational efficiency of our proposed approach. We hope the proposed CoIFNet framework and its theoretical justifications could inspire future research in related fields. Our code is available at: <https://github.com/KaiTang-eng/CoIFNet>.

REFERENCES

- [1] I. Price, A. Sanchez-Gonzalez, F. Alet, T. R. Andersson, A. El-Kadi, D. Masters, T. Ewalds, J. Stott, S. Mohamed, P. Battaglia *et al.*, “Probabilistic weather forecasting with machine learning,” *Nature*, vol. 637, no. 8044, pp. 84–90, 2025.
- [2] J. Zhang, F.-Y. Wang, K. Wang, W.-H. Lin, X. Xu, and C. Chen, “Data-driven intelligent transportation systems: A survey,” *IEEE Transactions on Intelligent Transportation Systems*, vol. 12, no. 4, pp. 1624–1639, 2011.
- [3] Y. Zhou, Z. Ding, Q. Wen, and Y. Wang, “Robust load forecasting towards adversarial attacks via bayesian learning,” *IEEE Transactions on Power Systems*, vol. 38, no. 2, pp. 1445–1459, 2023.
- [4] K. Zhang, Q. Wen, C. Zhang, R. Cai, M. Jin, Y. Liu, J. Y. Zhang, Y. Liang, G. Pang, D. Song, and S. Pan, “Self-supervised learning for time series analysis: Taxonomy, progress, and prospects,” *IEEE Transactions on Pattern Analysis and Machine Intelligence*, vol. 46, no. 10, pp. 6775–6794, 2024.
- [5] Y. Liu, T. Hu, H. Zhang, H. Wu, S. Wang, L. Ma, and M. Long, “itransformer: Inverted transformers are effective for time series forecasting,” in *Proceedings of the International Conference on Learning Representations*, 2024.
- [6] Y. Li and D. C. Anastasiu, “Mc-ann: A mixture clustering-based attention neural network for time series forecasting,” *IEEE Transactions on Pattern Analysis and Machine Intelligence*, 2025.
- [7] J. Wang, W. Du, Y. Yang, L. Qian, W. Cao, K. Zhang, W. Wang, Y. Liang, and Q. Wen, “Deep learning for multivariate time series imputation: A survey,” in *Proceedings of the International Joint Conference on Artificial Intelligence*, 2025.
- [8] X. Chen and L. Sun, “Bayesian temporal factorization for multidimensional time series prediction,” *IEEE Transactions on Pattern Analysis and Machine Intelligence*, vol. 44, no. 9, pp. 4659–4673, 2021.
- [9] C. Xu and Y. Xie, “Conformal prediction for time series,” *IEEE Transactions on Pattern Analysis and Machine Intelligence*, vol. 45, no. 10, pp. 11 575–11 587, 2023.
- [10] J. Zhang, L. Gao, X. Luo, H. Shen, and J. Song, “Deta: De-noised task adaptation for few-shot learning,” in *Proceedings of the IEEE/CVF international conference on computer vision*, 2023, pp. 11 541–11 551.
- [11] Y. Li, R. Yu, C. Shahabi, and Y. Liu, “Diffusion convolutional recurrent neural network: Data-driven traffic forecasting,” in *Proceedings of the International Conference on Learning Representations*, 2018.
- [12] B. Yu, H. Yin, and Z. Zhu, “Spatio-temporal graph convolutional networks: a deep learning framework for traffic forecasting,” in *Proceedings of the 27th International Joint Conference on Artificial Intelligence*, 2018, p. 3634–3640.
- [13] Y. Tashiro, J. Song, Y. Song, and S. Ermon, “CSDI: Conditional score-based diffusion models for probabilistic time series imputation,” in *Proceedings of the Advances in Neural Information Processing Systems*, 2021.
- [14] W. Cao, D. Wang, J. Li, H. Zhou, L. Li, and Y. Li, “Brits: Bidirectional recurrent imputation for time series,” in *Proceedings of the Advances in Neural Information Processing Systems*, vol. 31, 2018.
- [15] Y. Luo, X. Cai, Y. Zhang, J. Xu *et al.*, “Multivariate time series imputation with generative adversarial networks,” in *Proceedings of the Advances in Neural Information Processing Systems*, vol. 31, 2018.
- [16] X. Chen, X. Li, B. Liu, and Z. Li, “Biased temporal convolution graph network for time series forecasting with missing values,” in *Proceedings of the International Conference on Learning Representations*, 2024.
- [17] C. E. Shannon, “A mathematical theory of communication,” *The Bell system technical journal*, vol. 27, no. 3, pp. 379–423, 1948.
- [18] B. K. Nelson, “Time series analysis using autoregressive integrated moving average (arima) models,” *Academic Emergency Medicine*, vol. 5, no. 7, pp. 739–744, 1998.
- [19] F. A. A. Bashir and H.-L. Wei, “Handling missing data in multivariate time series using a vector autoregressive model-imputation (var-im) algorithm,” *Neurocomputing*, vol. 276, pp. 23–30, 2018.
- [20] B. N. Oreshkin, D. Carpio, N. Chapados, and Y. Bengio, “N-BEATS: Neural basis expansion analysis for interpretable time series forecasting,” in *Proceedings of the International Conference on Learning Representations*, 2020.
- [21] Z. Wu, S. Pan, G. Long, J. Jiang, and C. Zhang, “Graph wavenet for deep spatial-temporal graph modeling,” in *Proceedings of the 28th International Joint Conference on Artificial Intelligence*, 2019, p. 1907–1913.
- [22] L. Bai, L. Yao, C. Li, X. Wang, and C. Wang, “Adaptive graph convolutional recurrent network for traffic forecasting,” in *Proceedings of the Advances in Neural Information Processing Systems*, vol. 33, 2020, pp. 17 804–17 815.
- [23] Z. Wu, S. Pan, G. Long, J. Jiang, X. Chang, and C. Zhang, “Connecting the dots: Multivariate time series forecasting with graph neural networks,” in *Proceedings of the 26th ACM SIGKDD International Conference on Knowledge Discovery & Data Mining*, 2020, pp. 753–763.
- [24] A. Zeng, M. Chen, L. Zhang, and Q. Xu, “Are transformers effective for time series forecasting?” in *Proceedings of the AAAI Conference on Artificial Intelligence*, vol. 37, no. 9, 2023, pp. 11 121–11 128.
- [25] Z. Shao, Z. Zhang, F. Wang, W. Wei, and Y. Xu, “Spatial-temporal identity: A simple yet effective baseline for multivariate time series forecasting,” in *Proceedings of the 31st ACM International Conference on Information & Knowledge Management*, 2022, pp. 4454–4458.
- [26] H. Zhou, S. Zhang, J. Peng, S. Zhang, J. Li, H. Xiong, and W. Zhang, “Informer: Beyond efficient transformer for long sequence time-series forecasting,” in *Proceedings of the AAAI Conference on Artificial Intelligence*, vol. 35, no. 12, 2021, pp. 11 106–11 115.
- [27] H. Wu, J. Xu, J. Wang, and M. Long, “Autoformer: Decomposition transformers with auto-correlation for long-term series forecasting,” in *Proceedings of the Advances in Neural Information Processing Systems*, vol. 34, 2021, pp. 22 419–22 430.
- [28] Y. Nie, N. H. Nguyen, P. Sinthong, and J. Kalagnanam, “A time series is worth 64 words: Long-term forecasting with transformers,” in *Proceedings of the International Conference on Learning Representations*, 2023.
- [29] T. Zhou, P. Niu, L. Sun, R. Jin *et al.*, “One fits all: Power general time series analysis by pretrained lm,” in *Proceedings of the Advances in Neural Information Processing Systems*, vol. 36, 2023, pp. 43 322–43 355.
- [30] Q. Ma, Z. Liu, Z. Zheng, Z. Huang, S. Zhu, Z. Yu, and J. T. Kwok, “A survey on time-series pre-trained models,” *IEEE Transactions on Knowledge and Data Engineering*, 2024.
- [31] M. Jin, S. Wang, L. Ma, Z. Chu, J. Y. Zhang, X. Shi, P.-Y. Chen, Y. Liang, Y.-F. Li, S. Pan *et al.*, “Time-llm: Time series forecasting by reprogramming large language models,” in *Proceedings of the International Conference on Learning Representations*, 2024.
- [32] M. Liu, H. Huang, H. Feng, L. Sun, B. Du, and Y. Fu, “Pristi: A conditional diffusion framework for spatiotemporal imputation,” in *Proceedings of the 39th IEEE International Conference on Data Engineering*, 2023, pp. 1927–1939.
- [33] W. Du, D. Côté, and Y. Liu, “Saits: Self-attention-based imputation for time series,” *Expert Systems with Applications*, vol. 219, p. 119619, 2023.
- [34] Z. Che, S. Purushotham, K. Cho, D. Sontag, and Y. Liu, “Recurrent neural networks for multivariate time series with missing values,” *Scientific Reports*, vol. 8, no. 1, p. 6085, 2018.
- [35] Y. Rubanova, R. T. Chen, and D. K. Duvenaud, “Latent ordinary differential equations for irregularly-sampled time series,” in *Proceedings of the Advances in Neural Information Processing Systems*, vol. 32, 2019.
- [36] M. Schirmer, M. Eltayeb, S. Lessmann, and M. Rudolph, “Modeling irregular time series with continuous recurrent units,” in *Proceedings of the International Conference on Machine Learning*, 2022, pp. 19 388–19 405.
- [37] Z. Wang, L. Yang, L. Sun, Q. Wen, and Y. Wang, “Task-oriented time series imputation evaluation via generalized representers,” in *Proceedings of the Advances in Neural Information Processing Systems*, 2024.
- [38] J. Peng, M. Yang, Q. Zhang, and X. Li, “S4m: S4 for multivariate time series forecasting with missing values,” in *Proceedings of the International Conference on Learning Representations*, 2025.
- [39] C. Yu, F. Wang, Z. Shao, T. Qian, Z. Zhang, W. Wei, Z. An, Q. Wang, and Y. Xu, “GinAR+: A Robust End-To-End Framework for Multivariate Time Series Forecasting with Missing Values,”

- IEEE Transactions on Knowledge and Data Engineering*, no. 1, pp. 1–14, 2025.
- [40] K. Liang, Y. Liu, S. Zhou, W. Tu, Y. Wen, X. Yang, X. Dong, and X. Liu, “Knowledge graph contrastive learning based on relation-symmetrical structure,” *IEEE Transactions on Knowledge and Data Engineering*, vol. 36, no. 1, pp. 226–238, 2023.
 - [41] J. Deng, X. Chen, R. Jiang, D. Yin, Y. Yang, X. Song, and I. W. Tsang, “Disentangling structured components: Towards adaptive, interpretable and scalable time series forecasting,” *IEEE Transactions on Knowledge and Data Engineering*, 2024.
 - [42] T. Kim, J. Kim, Y. Tae, C. Park, J.-H. Choi, and J. Choo, “Reversible instance normalization for accurate time-series forecasting against distribution shift,” in *Proceedings of the International Conference on Learning Representations*, 2021.
 - [43] C. Wang, Q. Qi, J. Wang, H. Sun, Z. Zhuang, J. Wu, and J. Liao, “Rethinking the power of timestamps for robust time series forecasting: A global-local fusion perspective,” in *Proceedings of the Advances in Neural Information Processing Systems*, 2024.
 - [44] *Entropy, Relative Entropy, and Mutual Information*. John Wiley & Sons, Ltd, 2005, ch. 2, pp. 13–55.
 - [45] M. Van Ness, T. M. Bosschieter, R. Halpin-Gregorio, and M. Udell, “The missing indicator method: From low to high dimensions,” in *Proceedings of the 29th ACM SIGKDD Conference on Knowledge Discovery and Data Mining*, 2023, p. 5004–5015.
 - [46] H. Cheng, Q. Wen, Y. Liu, and L. Sun, “Robusttsf: Towards theory and design of robust time series forecasting with anomalies,” in *Proceedings of the International Conference on Learning Representations*, 2024, pp. 1–28.